Title
Systems Biology Approaches for Identifying Synthetic Lethal Targets in Cancer

Author
Ku, Angel Alejandro

Publication Date
2019

Peer reviewed|Thesis/dissertation

Systems Biology Approaches for Identifying Synthetic Lethal Targets in Cancer

by
Angel A. Ku

DISSERTATION
Submitted in partial satisfaction of the requirements for degree of
DOCTOR OF PHILOSOPHY

in

Pharmaceutical Sciences and Pharmacogenomics

in the

GRADUATE DIVISION
of the
UNIVERSITY OF CALIFORNIA, SAN FRANCISCO

Approved:

DocuSigned by:
Sourav Bandyopadhyay
F1E602E27884493...

Sourav Bandyopadhyay
Chair

DocuSigned by:
Frank Mccormick

Frank Mccormick

DocuSigned by:
Kevan Shokat
8FDF47C586EF40D...

Kevan Shokat

Committee Members

Acknowledgments

I would like to thank members of the Bandyopadhyay lab both past and present. Over the past five years it was a great pleasure having the support and advise from this group of scientists. I would also like to thank members of the UCSF community post-docs, grad students and summer students who made my time at UCSF memorable. I would also like to thank members of the McCormick lab for the useful discussions and assistance with experiments.

I would like to thank Sourav for his advice and mentorship, working with him was a great pleasure and I learned a lot from him. I would also like to thank PSPG faculty Nadav Ahituv, who has provided much guidance and support before and during my time at UCSF as a graduate student. Deanna Kroetz and Estaban Burchard for their key advise and support early in the graduate program.

I also would like to thank my friends and family outside UCSF. Elisa, my wife for her amazing support and encouragement during challenging times. My parents, Angel and Maria for their love and support and understanding during my journey at UCSF. Finally, I would like to thank my siblings Cindy and Diego for their encouragement and support.

Contributions

Some Chapters in this dissertation contain material that has been published previously. They do not necessary represent the final published form and in most case have been edited slightly.

Chapter 3 is a partial reprint of material in submitted for review:
AA Ku, S Kongara, H Hsien-Ming, X Zhao, D Wu, F McCormick, A Balmain, S Bandyopadhyay. “Integration of pathway, cellular and genetic context reveals principles of synthetic lethality that affect reproducibility”

Systems Biology Approaches for Identifying Synthetic Lethal Targets in Cancer

Angel A. Ku

Abstract

The development of therapeutic agents against cancer is based on targeting key signaling proteins that tumors highjack and use to survive. Although progress has been made to define cancer's vulnerabilities, a subset of cancer drivers remain undruggable. To address this problem the field has attempted to identify drug targets that would selectively kill cancer cells and spare wild type tissue, a concept known as synthetic lethality. My work here seeks to address major challenges in identifying synthetic lethal targets. First, I provide an overview of the platforms for synthetic lethal screening methodologies and considerations for screening. Chapter three is focused on a case study where we developed a network-based integration method for published KRAS synthetic lethal studies and derived principles that affect reproducibility. The major findings of this study highlight principles of synthetic lethal screening and identify a subset of genes, which may offer new therapeutic targets in the context of oncogenic KRAS. Chapter four explores the response of PARP inhibitors to a non-small cell lung cancer cell panel and I derive molecular signatures associated with response and resistance to PARP inhibitor. Chapter 5 summarizes the results of a KRAS 4a/4b drug screen that uncovered isoform specific vulnerabilities that may have implications for the use of MEK inhibitors in KRAS mutant cancers.

Table of Contents

List of Figures

Chapter 1: Introduction

1.1 Challenges to targeting cancer in the era of targeted therapies

Cancer is a complex disease driven by dysregulation of pathways that allow normal cells to break free of tumor suppressor and constitutively activate oncogenes[1]. A simplistic view of cancer suggests that targeting oncogenic drivers would be sufficient to halt tumor growth; however, tumors are highly dynamic and are able to adapt and overcome therapies[2]. Therefore, to effectively target tumors, we must understand the vulnerabilities and the adaptive mechanisms that can render therapies ineffective over time[3].

Seminal studies using viral vectors initially discovered a subset of genes that transformed NIH/3T3 cells and conferred outgrowth[4]. With the advent of whole genome sequencing the field applied these tools to the study the genomes of tumors. This approach reveled recurring mutations in tumors, which not surprisingly were the same set of oncogenes revealed in earlier studies[5]. Several studies supported that these oncogenes were necessary for tumor growth, which motivated the development of chemical agents to inhibit the kinase activity of these tumors. The generally principle has held up for and Bcr-Abl fusion oncogene and mutant EGFR in which mutations in the kinase domain were targetable through inhibitors like gleevec and gefitinib respectively[6]. However, there are three major limitations to this approach: 1) tumors

with no obvious oncogenic drivers 2) oncogenic proteins that have no clear targetable pockets and 3) the emergence of resistance to initial drug treatments[2].

1.2 Targeting KRAS Mutant Tumors

Mutations in the KRAS oncogene are present in 30% of all human cancers and are required for tumor development and maintenance in many tumor types[7]. There are three major areas of research that have emerged to targeting KRAS: 1) blocking the post-translational modifications (PTMs) required for localization KRAS protein to the plasma membrane 2) blocking downstream effectors of KRAS 3) and combination strategies. KRAS requires PTM to be properly shuttled to the cell membrane where it can be activated. Early studies focused on developing inhibitors to block the PTMs, but due to compensatory pathways this strategy was not viable[8,9]. Focusing on downstream KRAS effectors, MEK and PI3K have been the focus for targeting KRAS mutant cancers. MEK inhibitors were developed to block activation of the MAPK pathway which is required for cell survival and proliferation; however, while promising preclinical data supported this strategy, there has been no major benefit again in clinical settings[10]. Finally, the combination of MEK and PI3K inhibitors have been proposed, but it remains unclear of the toxicology profiles of these two drugs will be tolerated in patients[11].

An alternative approach to targeting KRAS directly is to selectively kill tumor cells harboring mutations in KRAS through the identification of alternative pathways that are required in KRAS mutant tumor cells but are otherwise non-essential in normal cells.

This approach, termed synthetic lethality, is an exciting approach to indirectly target this 'undruggable' oncogene.

1.3 Synthetic Lethality

Synthetic lethality is when a single knock down a gene is viable, but inhibition of both is lethal[12]. In the context of cancer therapeutics, it describes a condition where one gene is mutated and inhibition of a second gene kills cells with the first mutation. The current standard for synthetic lethality in cancer is the loss of PARP1 in BRCA1 mutant cells. Through the loss of BRCA1, cell are dependent in alternative pathways to repair DNA such as Non-Homologous End Joining (NHEJ) and thus inhibiting PARP1, a NHEJ gene completely abolishes a tumors ability to repair damaged DNA[13]. These finding have led to the development and approval of PARP inhibitors for BRCA1 mutant breast and ovarian cancers[14,15].

The BRCA1 PARP1 model has inspired several systematic approaches to target KRAS mutant cancers pathways through targeted and genome-scale RNAi screens to identify Synthetic Lethal (SL) genes[16–21]. However, all these studies so far have been unsuccessful in identifying effective clinical therapies for patients with KRAS mutations. The results of these studies have been a set of non-overlapping SL candidates that do not point to any obvious common targets[22]. Given the discordance between previous studies, the identification of vulnerabilities in KRAS cancers remains a major question in the field. Additionally, a systematic re-analysis of previously published has not been conducted which may reveal new insights into. And while advances in screening

technologies (i.e. CRISPRi) are set for the next generation our basic understanding of synthetic lethality in the context of cancer is still limited[23].

1.4 Future Directions

There has been great progress in the technologies for synthetic lethal screening; however, there is a gap to define principles for identifying synthetic lethal targets. Studies from model organism suggest that synthetic lethal targets are context dependent, and thus future work should focus on understanding how contexts governs synthetic lethality in order to define better and robust therapeutic targets.

Chapter 2: Methodologies for Synthetic Lethal Screening

2.1 Abstract

Genetic interaction mapping was initially used to study pathway structure in model organism and one type of interaction from these screens were negative or synthetic lethal (SL) interaction. Negative genetic interactions are of major interest for cancer research in order to identify mutation specific vulnerabilities. There is a wide array of tools and methods for identifying SL in cancer. In this review, I will discuss the use of RNAi technologies, including CRISPR platforms to define new therapeutic targets for genetically defined cancers. I will also discuss the use of chemical genetic screens to combat drug resistance and define novel combination therapies for cancer. Finally, I will highlight some key consideration when screening in order to account best define the biological contexts where SLs are present.

2.2 Target Identification through loss of function approaches

The methodologies used for exploring the vulnerable in cancer started with the advent of RNA interference (RNAi) technologies that allowed for the high throughput screening of mammalian cell lines. RNAi technologies generally fall under two categories: siRNAs and short-harpin RNA (shRNA) libraries[24]. siRNA are synthetic RNAs which target mRNAs and this siRNA/mRNA complex is process by the RISC complex which degrades the target mRNA. siRNA are transfected into cells and often have more than one oligo targeting the same mRNA in order to test multiple siRNA oligos and control for off target effects. Short harpin RNA (shRNAs) libraries are usually lentiviral, and each vector will express and shRNA that will be processed by Dicer/Ago complex to make a mature siRNA and the RISC complex to silence the target transcript. The workflow for shRNA requires generate lentivirus pools for all hairpin-containing vectors to infect a population of cells. Stable shRNA expressing cells are selected for through antibiotic treatment and then allowed to proliferate for several days. The basic principle of this approach depends on the “drop out” of cells where the knock down of genes are lethal. DNA is harvested from the cells and prepared for sequencing by amplifying the barcodes in the vectors. Given that a library was prepared at earlier timepoints it is possible to identify which shRNA dropped out or enriched over time. While these were the first tools to screen for synthetic lethal targets there were major issues with off target effects and knock down efficiencies[25]. However, advances in RNAi have allowed for the

development of new flavors of siRNAs, for example esiRNAs are endoribonuclease treated siRNAs, which allow for the transfection of short and heterogeneous population of short siRNAs target the same mRNA[26].

A major breakthrough in functional genomics occurred through the discovery and engineering of the Cas9 proteins for gene perturbation screens. There are two approaches for loss of function screen with CRISPR: 1) the first is to use the native protein to cut target genes to disrupt the sequence 2) through modified CRISPR proteins (dCas9-KRAB) that enabled the silencing of genes through fusing KRAB (Kruepple-associated box) domains to the modified Cas9 protein[27]. An attractive feature of these approaches is that gene expression silencing occurs at transcription, which increases the efficacy of knock-down and minimizes off target effects. Furthermore, as long as a cell stably expresses the dCas9-KRAB protein, a pooled screen can be conducted by lentivirally introducing a guide RNA library. For the most part CRISPRi screens have been conducted in non-adherent K562 cell lines, but these technologies are quickly being adapted to other cancer cell line models. While these technologies continue to evolve an emerging concern with the CRISPR system is the off target effects, however, this is likely to only affect the traditional CRISPR screens versus the CRISPRi approach[28]. In summary, we are reaching a point where our gene pertubation technologies are robust and optimized, which opens several opportunities for synthetic lethal screening as well as revisiting former challenging problems in this area of research.

2.3 Genetic interaction maps to uncover resistance mechanism to targeted therapies.

Once a target has been identified a reasonable question to ask is: what are the genes that can alter the response to the primary target. There are several methods to ask this question, but here I will focus my discussion on chemical-genetic approaches to combat resistance to targeted therapies. An example of this approach has been in the context of MEK inhibitors. While MEK inhibitor showed great preclinical efficacy, human trails have shown that there is no added benefit to MEK inhibitor in the context of KRAS mutant cancers[10]. One potential hypothesis is that there are other genetic factors beyond KRAS mutations and may govern response to MEK inhibitors. Two studies have shown that ERBB2 and FGFR1 expression confer resistance to MEK inhibitors, the study by Sun and colleagues implicated FGFR1 through a MEK inhibitor plus shRNA screen[29,30]. This approach has also been used to systematic test dozens of drugs and genetic factors in ovarian and breast cancer, the end result which was a chemical-genetic map of chemotherapies[31]. A CRIPSR/olaparib screen identified RNA-DNA lesions as another source of PARP lesions which was previously an unknown mechanism contributing to PARP sensitivity[32]. Taken together these findings highlight that chemical-genetic approaches are capable of identifying factors that contribute to resistance and sensitivity to targeted agents. As more drug targets are identified through SL screening, complementing the results with chemical-genetic screen can support development of

therapeutic strategies to better define the patient populations that will be at relapse or respond to therapies.

2.4 Considerations for SL Screening

2.4.1 Cell Lines:

Cell lines are the battleground we apply our gene perturbation technologies and thus it is important to consider early what is the best platform for the research question on hand. There are generally two options for screening: isogenic pairs and cancer cell line panels. Isogenic cells, offer defined genetic background to start that can aid in identifying mutation specific vulnerabilities[33]. However, the major caveat is that isogenic cell line may not be representative of tumors, but if exploring the nuances of genetic interaction in defined genetic background is the question being considered this is a reasonable approach. A popular tool for studying MAPK signaling is using NIH/3T3 mice cells[4]. In the absence of growth factors these cells do not proliferate, however upon introducing oncogenic KRAS cells proliferate in the absence of factors. In a similar vein, mammary epithelial cell line MCF10as have also been used to study the signaling profiles and therapeutic vulnerabilities of oncogenes[34,35]. The advantage of these oncogene “add in” platforms is that removing growth factors allows for a system were proliferation is driven by the introduction oncogenes, which provide a positive control through genetic or chemical inhibition of the oncogene.

In comparison cell line panels offer a heterogeneous panel of cells which can be screen in order to identify subsets which respond to an inhibitor[36]. Systematic efforts to classify drug sensitivity across cell lines have been conducted by the CCLE and the Broad Institute along with other 'Omic' (RNA-seq, DNA-seq) characterization of the cell lines[37–39]. However, a major challenge in these efforts have been those of reproducibility of findings across different laboratories[40]. Nevertheless, cell lines do offer diverse panels of cells which can aid in defining responder and non-responder subsets.

2.4.2 Growth Conditions

Context dependency has been attributed to the failure to identify robust SL targets for genetically defined cancers[23,41]. However, I argue that context is an innate feature of genetic interactions. Studies from model organism show that essential genes between two strains of yeast often do not overlap, which suggest than in tumors that are constantly evolving that a drug target may not be viable over time or across tumors with minor difference in genomic backgrounds[42]. Therefore, SLs hits from primary screens should be framed as a starting point for therapeutic strategies and elucidating the context that preserve or mask these types of interaction should be explored. Work by Bandyopadhyay and colleagues have highlighted the context dependency of genetic interactions. The study showed that 70% of the positive genetic interactions in the presence of MMS were not observed in the untreated conditons[43]. This highlights the highly plastic nature of genetic interactions and suggests that only subsets of genetic interactions are preserved.

2.5 Conclusion

The toolkit of functional genomics is greatly expanding through the ability to use CRISPR expand genetic backgrounds to explore. This will allow for the development of isogenic cell lines where we can begin to test the robustness of synthetic lethal targets against relevant mutations. Furthermore, RNAi technologies are quickly becoming more efficient and robust which allow for higher dimensional screens where we can test a library across dozens of growth of mutational backgrounds. Chemical-genetic are able to take our drug targets of interest and further test the genetic factors important for mediating drug resistance. The next hurdle in making precision medicine a reality will be in identifying the “contexts” altering synthetic lethality. Fundamental studies have been conducted to characterize the nature of genetic interactions across growth conditions and genetic background, but we will also need to consider other factors that are relevant to tumor biology. This will require investigators to develop high throughput assays that mimic tumor microenvironments, and tumor-immune interactions in order to account for these emerging themes in synthetic lethality.

Chapter 3: Integration of pathway, cellular and genetic context reveals principles of synthetic lethality that affect reproducibility

3.1 Abstract

Synthetic lethal screens have the potential to identify new vulnerabilities incurred by specific cancer mutations but have been hindered by lack of agreement between studies. Using KRAS as a model, we identified that published synthetic lethal screens significantly overlap at the pathway rather than gene level. Analysis of pathways encoded as protein networks identified synthetic lethal candidates that were more reproducible than those previously reported. Lack of overlap likely stems from biological rather than technical limitations as most synthetic lethal phenotypes were strongly modulated by changes in cellular conditions or genetic context, the latter determined using a pairwise genetic interaction map that identified numerous interactions that suppress synthetic lethal effects. Accounting for pathway, cellular and genetic context nominates a DNA repair dependency in KRAS-mutant cells, mediated by a network containing BRCA1. We provide evidence for why most reported synthetic lethals are not reproducible which is addressable using a multi-faceted testing framework.

3.2 Introduction

Synthetic lethality is a type of genetic interaction that occurs when the simultaneous perturbation of two genes results in cell death. Such an approach has been used to define new vulnerabilities in cancer cells harboring defined mutations, such as the case of BRCA1- or BRCA2- mutant cells which are sensitive to PARP inhibition [13,44]. In search of such vulnerabilities, functional genomic screens have enabled the rapid mapping of potential synthetic lethal relationships using isogenic or collections of cell lines harboring specific mutations of interest. Although experimental technologies to map synthetic lethality such as those using shRNA and CRISPR-pooled screens are rapidly scalable, significant challenges remain that limit the utility of using high throughput approaches for the development of new synthetic lethal therapies. It has been suggested that the predominant barrier to identifying relevant synthetic lethals is that of interaction penetrance, or resiliency against modulation by additional genetic changes found in cancers, also called “hard” versus “soft” synthetic lethality [23,45]. Computational and experimental strategies geared toward overcoming this challenge are largely unexplored.

KRAS is the most commonly mutated oncogene in cancer. It is as yet undruggable, activates a variety of signaling pathways, and is exemplary to the challenges in identifying synthetic lethals. While a multitude of studies have sought to define KRAS synthetic lethal genes [16–19,46,47], they have been notable for the fact that they hardly overlap, which has been attributed to the use of different cell lines and screening libraries that may suffer from off-target effects and partial knockdowns [22]. As a result,

many of the published synthetic lethal genes that have been explored independently have failed to reproduce [48,49]. While a meta-analysis of published synthetic lethals could be an effective way to identify more robust candidates, a systematic integration and re-testing has not yet been performed [22,50].

The bulk of our knowledge of the organization of genetic interactions comes from model organisms through single and combination knockout studies [42]. Large scale mapping of such interactions, including synthetic lethals, have been found to link functionally related proteins and used to delineate pathway structure [51,52]. Genetic interactions have been shown to be highly context specific with changes in environment and strain dramatically altering pathway usage and synthetic lethal relationships in yeast [43,53]. The plasticity of genetic interactions present in single-celled organisms likely foreshadows the challenges in the identification of clinically relevant synthetic lethal interactions in a heterogeneous disease such as cancer.

We hypothesized that challenges in identifying synthetic lethal interactions stems from the fact that differences in gene dependencies among cancer cells parallel the widespread differences in gene essentiality observed in model organisms that are exposed to environmental or genetic changes [42,53]. Integrating across studies, we show that previously published KRAS synthetic lethal screens contain significant information regarding the pathways required for KRAS mutant cells in a manner that extends beyond the single gene that is often reported. Genes involved in these pathways were more likely to be recapitulated in confirmatory studies, indicating that they are more

likely to be context-independent. Further testing of synthetic lethal genes identified that most were profoundly influenced by changes in cellular conditions and presence of genetic modifiers, likely explaining why published synthetic lethals have had limited utility. Accounting for context highlights a DNA repair pathway as a dependency in KRAS mutant cancers, which was reproducibly observed in multiple studies but not always the top hit and therefore not immediately apparent. We delineate why most synthetic lethal interactions are not reproducible, and define a new approach to process and integrate synthetic lethal screens to identify context-independent genetic interactions that operate at the level of a pathway rather than a single gene.

3.3 Results

3.3.1 Meta-analysis of published KRAS synthetic lethal screens identifies reproducible synthetic lethal networks

The concept of synthetic lethality is a powerful tool to identify new dependencies and gene targets in cancer, but despite their potential their utility has been limited by challenges in robustness and reproducibility related to cellular context [22,23,41,54]. We hypothesized that integrating multiple independent studies may reveal synthetic lethal interactions that are independent of cellular context and hence more reproducible. To determine the degree to which this was the case, we analyzed three seminal studies which sought to define KRAS synthetic lethal genes through loss of function screens, hereafter called the Luo, Barbie and Steckel studies [17,19,20]. The Luo and Steckel studies

used unique pairs of isogenic cells whereas the Barbie study used a panel of KRAS mutant and wild-type cell lines. As a basis for comparison we selected the top 250 KRAS synthetic lethal genes reported in each study as hits (KSL genes, Table 1), and found that there was marginal overlap between any pair of studies based on a hypergeometric test accounting for total number of tested genes in each study, consistent with previous reports (Figure 3.1A) [22,50]. We next explored whether each screen could have identified distinct but related genes, indicating shared essentiality at the pathway rather than gene level. For example, different subunits of the 26S proteasome (PSMB6, PSMD14) were identified by different studies [22], suggesting convergence between studies at the pathway level (Figure 3.1A). We integrated these gene lists with a protein-protein interaction (PPI) network comprising known protein complexes from CORUM and high confidence physical and functional interactions from HumanNet [55,56]. In total we identified 6,830 interactions involving a protein product of a KSL gene from any of the three studies (Figure 3.1B). We found 260 interactions connecting KSL genes found in different studies. To assess if this was a significant number we compared the number of interactions spanning between pairs of studies to the number of interactions expected among randomly selected gene sets, controlling for sample size and test space (see Methods). In all cases, we observed significantly more connections between KSL genes from two independent studies than expected at random (Figure 3.1C). For example, we observed 162 PPIs between the top 250 genes in the Luo and Steckel studies, which was approximately 8-fold higher than expected between 250 random genes, representing a $p<0.0001$. In contrast, the gene level overlap between these two studies was not significant ($p=0.17$) (Figure 3.1A).

Since KSL genes from different studies were enriched to interact functionally and physically, we next asked if they converge into molecular sub-networks representing known pathways and protein complexes. We applied a network clustering algorithm called MCODE on this network to identify dense gene sub-networks, or modules, enriched with KSL genes spanning multiple studies [57]. Based on our requirement that a subnetwork must include a gene found in two or more studies, we identified 7 functionally distinct KRAS synthetic lethal networks, all of which could be traced back to a specific protein complex or pathway (Figure 3.1D, Table 2A). For example, one of the networks corresponds to the Proteasome and Anaphase promoting complex (CORUM ID: 181 & 96), which includes subunits encoded by genes identified in the Luo, Barbie and Steckel studies (Figure 3.1D). Other complexes and pathways we identified in this study were the Nop56p-associated pre-rRNA complex (containing Steckel and Luo genes), BRCA1-RNA polymerase II complex (Steckel and Barbie), the RC complex during S-phase of the cell cycle (all three studies), LCR-associated remodeling complex also called LARC (all three studies), the Chaperonin containing TCP1 complex also called CCT (Luo and Steckel) and the Insulin signaling pathway (Steckel and Barbie). In all cases, these complexes and pathways were significantly enriched for KSL genes (Figure 3.1D). In total we predicted 105 KRAS synthetic lethal network genes (Network SL genes), of which 65% (68/105) were not covered in our original KSL lists (Figure 3.1D, Table 2, 3). Hence, despite the limited gene level overlap in published studies, network integration reveals that independent KRAS synthetic lethal studies converge on shared protein complexes and pathways.

3.3.2 KRAS synthetic lethal networks gene are more like to be hits in other published studies

Since our network analysis highlighted shared pathways and complexes across studies, we hypothesized that Network SL genes may represent synthetic lethals that are more robust, and hence more likely to be reproduced in follow up studies. To address this we asked if they were more likely to be recovered in a series of more recent RNAi screens that were not used for network identification as compared to 26 previously published KRAS synthetic lethal genes curated from the literature (Literature SL) (Table 2B) [16,46,47]. Both Kim et al. 2013 [46] and Kim et al. 2016 [47] studies used panels of KRAS mutant versus wild-type lung cancer lines, and the Costa-Cabral study [16] used an isogenic panel of colorectal cancer lines. To facilitate comparison, we independently ranked genes identified from each of these three studies into percentiles, with genes in the lowest percentile showing the strongest evidence of KRAS synthetic lethality (see Methods). Network SL genes were more likely to be among the top percentile of hits than Literature SL genes previously published. For example, in the Kim et al 2016 study, 15% of the Network SL genes tested were in the top one percentile of hits as compared to 3% of Literature SL genes, a 5-fold increase (Figure 3.2). Similarly, 9% of Network SL genes were in the top 1% of hits in the Kim et al. 2013 study, compared to 0% using Literature SL genes. Network SL genes also predicted the top candidate from the Costa-Cabral study, CDK1. Taken together as a meta-analysis of six studies, these data provide additional support for genes involved in the RC complex during S-phase

(CDK1, RPA1, RPA2) and the BRCA1-RNA polymerase II complex (POLR2B, POLR2D, POLR2G, BRCA1) as KRAS synthetic lethal candidates that were repeatedly replicated in multiple studies. Hence a network approach to identifying synthetic lethal genes based on their pathway context identifies reproducible synthetic lethals in a manner that is superior to the standard single study, single gene approach.

3.3.3 Evaluation of published and predicted KRAS SLs in an isogenic KRAS dependency model.

We next sought to obtain independent experimental evidence that the incorporation of pathway context could identify robust KRAS synthetic lethals. We established an isogenic model using MCF10A cells expressing KRAS G12D or eGFP as control and screened them in parallel using an arrayed gene knockdown library independently targeting 28 Literature SL genes, 40 Network SL genes and 128 genes in KRAS pathway (Figure 3.3A, Supplementary Figure 3.1S, Table 3). MCF10A cells are non-transformed and have been used extensively to model RAS signaling [34,35] and mutant KRAS is often amplified in human cancer, indicating the relevance of our approach [58,59]. KRAS G12D cells did not proliferate significantly more than control eGFP expressing cells and KRAS cells were growth factor independent and sustained MAPK activity in the absence of growth factor, a hallmark of oncogenic transformation and key feature of KRAS biology (Figure 3.3B,C). As positive control, we observed that knockdown of KRAS only reduced the proliferation of KRAS-expressing cells in the absence of all media supplements and growth factors (minimal media), demonstrating KRAS

dependency in this model (Figure 3.3D). Comparison of the proliferative impact of gene knockdown in control eGFP versus KRAS mutant cells grown in minimal media was used to define an interaction score related to the significance of effect over four replicates, with negative scores representing putative synthetic lethal hits (see Methods). Using a False Discovery Rate (FDR) cutoff of 5%, we identified 28 hits including KRAS (Figure 3.3E). Among the top 10 genes were predicted Network SL genes BRCA1 (S=-6.3) and RPA3 (S=-4.2), and previously described Literature SL genes GATA2 (S=-4.9), YAP1 (S=-2.9) and RHOA (S=-5.4) (Figure 3.3F). At the pathway level KRAS cells were notably dependent on genes in the RAS, ribosomal protein S6 kinase (S6K), cell cycle and YAP pathway (Figure 3G). Inhibition of receptor tyrosine kinase (RTK) signaling had the least effect on the KRAS cells, as typified by knockdown of GRB2, which links RTKs and RAS signaling, that was more toxic to eGFP than KRAS cells (S=5.9) (Figure 3.3F,G). Most hits were independent of the particular KRAS allele used as screening results between G12V and G12D expressing cells were highly correlated (r=0.81, Supplementary (Figure 3.2, Table 4). With respect to previously published Literature SL genes, we found that 6/27 (22%) were recovered at an FDR<10% but on average they did not have negative interaction scores consistent with synthetic sickness or lethality as a group (p=0.48 based on Student's t-test) (Figure 3.3I). In contrast, the 39 predicted Network SL genes as a group had overall strong negative scores (p=4.6e-5 based on Student's t-test) that were overall more negative than Literature SL genes (p=0.046), and 33% were synthetic lethal hits (13/39 at a FDR of 10%) (Figure 3.3I). Taking our retrospective analysis and new experimental data

together, our findings indicate that a network meta-analysis approach is an effective strategy to identify robust and reproducible synthetic lethal genes.

3.3.4 Dependency of KRAS synthetic lethals on genetic context

Limitations in gene knockdown technologies have been suggested to contribute to the lack of reproducibility of KRAS synthetic lethals and potentially resolved using CRISPR-based approaches [22]. Another explanation could be that synthetic lethal effects are incompletely penetrant and do not manifest equally in cells with different genetic backgrounds [23]. To establish the degree to which genetic context influences synthetic lethal identification and to elucidate targets that are resilient to this effect, we systematically screened for secondary perturbations that alter synthetic lethal phenotypes. We generated a quantitative epistasis map (E-MAP) through the systematic measurement and comparative analysis of the fitness of single and pairwise gene perturbations using RNA interference [60]. In this system, positive scoring interactions constitute buffering or epistatic interactions and occur when the effect of combination knockdown is less than what is expected given the two gene knockdowns separately, in the extreme case causing a complete suppression of the phenotype of one perturbation by the another [61,62]. Negative interactions indicate gene pairs that operate independently and when co-depleted produce a stronger phenotype than expected [61]. We generated an E-MAP in MCF10A KRAS G12D cells by knocking down the 31 of the top synthetic lethal genes we identified in our single gene study (query genes) in combination with 188 genes mostly involved in the broader RAS signaling

pathway (Figure 3.4A, Table 5). Together, we measured interactions among 5,828 gene pairs and identified 170 positive and 105 negative interactions at a score cutoff of 2 (Z>|2|) corresponding to two standard deviations from the mean (Figure 3.5B). At this score cutoff we found strong interactions occurring between 4.6% of gene pairs, consistent with observed genetic interaction rates in yeast [63].

For the 31 query genes we tested, we identified 170 genetic interactions that suppress their synthetic lethal phenotype in KRAS mutant cells (Z>2, average of 5.5 per gene). We validated several of the strongest hits in small-scale studies. For example, while CCND1 knockdown was selectively toxic to KRAS cells, co-knockdown of RASSF5 reverted KRAS mutant cells back to normal proliferation (Z=3.9) (Figure 3.4C). The impact of knockdown of CDK6 was also significantly rescued by knockdown of RASSF5 (Z=3.8) and ERBB2 (Z=3.3). Genetic modifiers could also modulate dependency on published KRAS synthetic lethal targets. For example, while knock down of STK33 was selectively toxic in KRAS G12D but not eGFP cells it was suppressed by simultaneous knockdown of SHP2 (Z=5.1) or ARID1B (Z=3.0) (Figure 3.4C). A pathway-based analysis identified 32 connections between query genes and cellular pathways where interactions could be organized as a bundle that were significantly positive or negative (p=0.05, Figure 3.4D, see Methods). For example, we identified that knockdown of RALGDS-Like 1 (RGL1) displayed positive interactions with genes involved in stress-linked MAPK, RHO, and RAC pathways (Figure 3.4D,E) and found largely negative interactions between DNA Methyltransferase 3 Alpha (DNMT3A) and the spliceosome and anaphase and proteasome complex (Figure 3.4E). These results demonstrate that

KRAS synthetic lethal gene inhibition may be suppressed by loss of secondary genes and pathways, in some instances completely rescuing lethal phenotypes.

3.3.5 Dependency of KRAS synthetic lethals on media complexity

Environmental differences such as variation in the growth factors and nutrients available in serum and media can alter cell biology [64,65] and have been postulated to contribute to challenges in validating candidate therapeutic targets in cancer [66]. We postulated that such changes in cellular context may be a potential source of the lack of durability in reported synthetic lethal genes in vitro. If correct, this could be a significant detriment to advancing synthetic lethal targets in vivo and in humans where such variability certainly exists in the complex tumor microenvironment. To model such changes, we iteratively added supplements back into the minimal media that was used in our initial screen to MCF10A KRAS G12D cells. To minimal media we added insulin, cholera toxin, and hydrocortisone (termed intermediate media) and found that it partially rescued cellular dependency on KRAS and further addition of EGF (full media) completely abolished KRAS dependency (Figure 3.5A). We performed parallel single gene knockdown screens using these three different conditions and found dramatic differences in the synthetic lethal interactions we observed (Figure 3.5B, Table 4). Strikingly, genetic interaction scores between experiments performed in minimal or intermediate media were weakly correlated and not significant ($r = 0.11$) (Figure 3.5B, Table 4).

We next explored the degree to which media conditions modulate the dependency on published KRAS synthetic lethal genes. We observed that synthetic lethality with members of the proteasome (e.g. PSMA2, PSMA5) [17,19] was only evident in cells that were grown in more complex media (and KRAS independent) suggesting that this pathway may only be necessary for KRAS-mutant cells when both KRAS and growth factor signaling are present (Condition Specific SLs, Figure 3.5C,D). Similarly, two published KRAS synthetic lethal genes, STK33 and YAP1, were only a dependency in minimal media conditions, but not in others providing a possible basis for why STK33 has been difficult to reproduce (Figure 3.5D) [18,67,68]. Of the 26 literature synthetic lethal genes we analyzed, the vast majority (92%) demonstrated synthetic lethality only in specific media conditions or not at all in the conditions we tested. Although most of the synthetic lethal relationships were specific to certain conditions, some were independent of condition and were consistent synthetic lethal interactions the strongest and most consistent of which were BRCA1 and RGL1 (Figure 3.5B,D). Together with our combinatorial genetic interaction map, these results demonstrate the dependence of most reported synthetic lethal genes on cellular and genetic context.

3.3.6 KRAS mutant cells are DNA repair deficient and PARP inhibitor sensitive

Our studies suggest that considering pathway, cellular and genetic context may help delineate robust synthetic lethal effects. We first developed a composite score based resiliency of a candidate SL gene based cellular and genetic context screens (Figure

3.6A, see Methods). Ranking 31 single synthetic lethal genes from our initial isogenic screen, we found that Network SL genes trended towards being more context independent than Literature SL genes ($p=0.05$ via rank sum test). This analysis identified the Network SL gene BRCA1 as a top candidate. Supporting this finding, our network meta-analysis identified two complexes involved in DNA repair and replication that included top hits from all three original RNAi studies including BRCA1 as well as POLR2G, POLR2D, POLR2B, RPA1, RPA2, RPA3 (Figure 3.1D). Six out of seven genes in this network were also found in the top 5% of hits from three additional studies (Figure 3.2). BRCA1 was the top hit in our single gene synthetic lethal screen, was a consistent synthetic lethal across media conditions (Figure 3.5B), and had a lower than average number of genetic suppressors (Suppl Figure 3.3S). Based on the function of BRCA1, we hypothesized that KRAS mutant cells harbor a unique dependence on DNA repair. We confirmed the dependency on BRCA1 in MCF10A-KRAS cells using independent siRNA reagents (Supp Figure 3.4S). We next sought further corroborative evidence of a DNA repair defect by identifying related chemically addressable vulnerabilities. An independent screen of 91 anti-cancer compounds highlighted several drugs targeting the DNA repair pathway as top hits in MCF10A KRAS G12D cells including WEE1, CHK1/2 and PARP inhibitors (Figure 3.6B, Table 6). We validated PARP inhibitor sensitivity using three different PARP inhibitors, with talazoparib showing a ~1,000 fold difference in IC_{50} between parental and KRAS mutant cells, and with rucaparib and olaparib demonstrating 2-5-fold sensitization (Figure 6C, D). These PARP inhibitors equally inhibit PARP enzymatic activity, but talazoparib most strongly traps it onto DNA causing DNA double strand breaks that are preferentially repaired by

homologous recombination via BRCA1 [69]. Hence these KRAS cells have a dependence on BRCA1 that creates a vulnerability to PARP inhibition and are preferentially sensitive to agents that trap PARP onto chromatin.

We hypothesized that KRAS mutant cells are defective in DNA repair resulting in a dependency on this pathway to maintain genome fidelity. At baseline, KRAS-mutant cell lines harbored more γH2AX foci, a marker of DNA double strand breaks, compared to control cells indicating that mutant KRAS induces DNA damage (Figure 3.6E, F). These results were independent of proliferation, as control and mutant cells grew at the same rate (Figure 3.3D). Treatment for 18 hours with talazoparib led to approximately equivalent amount of total DNA damage indicating that PARP inhibitors do not simply increase the induction double strand breaks in KRAS mutant cells (Figure 6G). In contrast, after wash out of the PARP inhibitor, KRAS cells had a delay in the resolution of double strand breaks that persisted for at least 24 hours indicating that KRAS causes a deficiency in the repair of double strand breaks caused by PARP inhibition (Figure 3.6G).

We sought to determine if sensitivity to PARP inhibitors was resilient against changes in cellular and genetic context, the same key features that led us to focus on BRCA1. Sensitivity to PARP inhibition in KRAS cells was independent of media conditions (Supplementary Figure 3.5S). Knockdowns of 191 genes against talazoparib treatment identified one suppressor, far lower than the number of suppressors associated with most of the genetic knockdowns in our study (Supplementary Figure 3.3S). Hence,

PARP inhibition demonstrates KRAS synthetic lethality that is robust to changes both in genetic and cellular context in this system. To determine if these findings extended to other models of RAS mutant cancer we analyzed cells derived from skin tumors initiated in mice using a dimethylbenz[a]anthracene (DMBA)-initiated and a 12-O-tetradecanoylphorbol-13-acetate (TPA)-promoted two-stage skin carcinogenesis protocol resulting in tumors that characteristically harbor an oncogenic HRAS mutation [70,71]. HRAS-mutant CCH85 carcinoma cells were sensitive to all three PARP inhibitors as compared to C5N keratinocytes controls with a 10-25 fold change in IC50 for talazoparib (Supplementary Figure 2-S6A) which was also corroborated in long term colony formation assays (Supplementary Figure 3.6S B). Next, we analyzed PARP inhibitor sensitivity in panels of cell lines derived from tumor types where RAS mutations are prevalent enough for statistical comparison in the genomics of drug sensitivity (GDSC) dataset which include colorectal, lung and ovarian cancer cell lines [37]. Among these tumor types, we identified numerous significant associations between KRAS mutation and olaparib sensitivity ($p<0.002$ for Colorectal and ovarian, $p=3e-6$ overall, (Supplementary Figure 3.6S C). Compared to other mutations or copy number associations present in the genome, KRAS mutation was often among the top genomic features associated with olaparib sensitivity (Supplementary Figure 3.6S D). We conclude that considering pathway, cellular and genetic context identifies a dependency on DNA repair that is targetable with PARP inhibitors warranting further investigation in other RAS-mutant cancers.

3.4 Discussion

The concept of synthetic lethality is an exciting approach to target cancer cells harboring specific cancer mutations that may otherwise be undruggable. We provide evidence for why most results from synthetic lethal studies have proven difficult to reproduce and offer a framework for identifying more robust synthetic lethal candidates. Recently improved genetic perturbation techniques such as those using CRISPR/Cas9 have led to renewed interest in synthetic lethal screening [72]. We argue that these technologies alone cannot intrinsically overcome limitations due to differences in cellular and genetic context present between cancer models. We provide key experimental evidence for and strategies to resolve the differences in genetic context that have been thought to contribute to failures in synthetic lethal identification [23,45].

Here we show that most synthetic lethals are highly dependent on cellular and genetic context. While testing published synthetic lethals we found that most were highly modified by cellular and genetic perturbations. For example, STK33 and GATA2 displayed synthetic lethality with KRAS only in a single isolated media condition and had among the most number of genetic suppressors. KRAS specific dependence on both these proteins has been disputed [67,68]. We propose computational and experimental approaches that we anticipate will identify more robust synthetic lethal interactions for further study. First, we provide a computational approach that enables the identification of synthetic lethals that are more context independent. This retrospective approach leverages pathway information to integrate functional genomics data as opposed to

previous work based on gene list analyses [22,50]. Second, we propose an experimental framework to rigorously test synthetic lethal effects using a panel of changes in cellular conditions as well as screening against a panel of secondary perturbations to determine genetic resiliency, potentially using an E-MAP approach. In addition to changes in media conditions, variation may also be achieved by modulating the environment (e.g. hypoxia), growth density and batch of cell lines used [73]. While our framework attempts to model the genetic and environmental heterogeneity present in cancers in a manner that is still amenable to high-throughput screening, future work could extend these approaches to vastly more secondary genetic perturbations as well as modulate the environment in different ways.

Applying our meta-analysis approach to three early KRAS screens we identified a set of networks representing protein pathways and complexes that were recurrently identified in different studies. Many components of these networks were found to re-validate in three held out studies and our isogenic model. Among these we investigated a network involved in DNA replication and repair. One component of this network, BRCA1, was a strong synthetic lethal regardless of cellular condition and had among the lowest number of genetic suppressors in our panel. The CCT complex, a chaperone complex involved in helping to fold part of the proteome [74], was also highlighted by our meta-analysis approach, and components of this complex were highlighted in 4 independent studies in total, warranting further investigation. This network framework enhances target discovery by accounting for pathway context in synthetic lethal screens to identify robust and potentially new targets for genetically defined cancers.

Our data highlight a potential role for PARP inhibitors in KRAS mutant cancers and warrants further investigation. PARP inhibitors inhibit PARP by both enzymatic inhibition as well as trapping PARP onto DNA and impairing replication during S-phase [69]. We observed the most differential inhibition of wild-type versus KRAS mutant cells with the strongest PARP trapper, talazoparib suggesting that KRAS cells are dependent on unencumbered progression through S-phase which is consistent with the role of the DNA replication network we identified. This interaction was also evident in a chemically induced murine tumor model and in small molecule profiling data across colorectal, lung and ovarian cancer cell lines tested for sensitivity to olaparib (Supplementary Figure 3.6S). Both enhancement [75] and suppression (Gilad et al., 2010; Kalimutho et al., 2017; Kotsantis et al., 2016) of DNA repair processes have been linked with mutant KRAS. These differences may be explained by the cell line panel profiling results, where although KRAS mutant cells tend to be more sensitive to PARP inhibitors on average, a subset are more drug resistant. Therefore, one possibility is that additional genetic contexts not investigated in this study may influence this synthetic lethal relationship and determining which KRAS mutant contexts predict dependence on specific DNA repair pathways will require future work. Such work may define the impact of changes in genetic context in terms of secondary mutations that co-occur with mutant KRAS, such as TP53 and LKB1, on PARP inhibitor sensitivity.

3.5 Methods

3.5.1 Synthetic lethal screen analysis

We obtained screen data from supplementary information from the Luo, Steckel and Barbie studies and ranked all genes based on the scoring criterion reported in the supplementary material from each manuscript. Since the Barbie study only reported 250 hits as significant, this cutoff was used for further analysis and all other studies reported >250 hits. Significance in overlap between gene sets was determined by calculating a hypergometric p-value of overlap between the top 250 genes from each study, and setting the background tested genes. The hypergeometric was 1-phyper(x, m, n, k) [79] [505150]with x as the overlap in hits between study 1 and study 2, m is the number of total genes tested in study 1, n is the number of hits found in study 2 that were also tested in study 1, k is the top 250 hit genes in study 1.

For the human protein-protein interaction (PPI) dataset we downloaded all CORUM protein complexes and HumanNet PPIs with scores > 3 to derive a list of high confidence PPIs. In order to identify highly connected subnetworks we applied the MCODE clustering algorithm with default parameters to this network in Cytoscape and considered clusters with genes that were reported in multiple KRAS SL studies for downstream analysis [57]. Clusters were analyzed using the gProfiler web tool [80] against the CORUM or the KEGG signaling pathway in order to functionally categorize clusters, with p-values of enrichment corrected for multiple testing. To determine the significance

in network based overlap between two KRAS studies we randomly selected 250 genes from the list of genes tested in each study and determined the number of interactions spanning genes from two studies to establish a null distribution. This null distribution was compared to the actual overlap observed between two studies to determine a p-value defined as the fraction of 10,000 random simulations that had more interactions than what was observed in the real data.

To compare gene sets in additional studies we used a percentile approach because of the subjectivity evaluating a p-value cutoff to select hits from screening data of different types (i.e. isogenic vs cell line panels). To perform evaluation in held out KRAS SL screen datasets we obtained gene level screening data from three published KRAS studies [16,46,47]. Hits were taken as ranked in the Costa Cabral study. For the Kim studies genes were ranked into percentiles based on the average difference in essentiality scores between KRAS wild-type and mutant cell lines.

3.5.2 Pathway Genetic Interaction Enrichment Analysis

Genes were assigned to curated pathways based on a combination of the RAS 2.0 pathway annotations (https://www.cancer.gov/research/key-initiatives/ras/ras-central/blog/2015/ras-pathway-v2) and manual curation. The significance of sets of genetic interactions between a gene and a particular pathway was evaluated using a two-sided t-test to determine significance from a median of zero.

3.5.3 Cell Lines & Tissue Culture

MCF10A Isogenic cells were grown in three conditions for our experiments. Full Media defined as: DMEM/F12, 5% Horse Serum, 20ng/ml EGF, 0.5mg/ml Hydrocortisone, 100ng/ml Cholera Toxin, and 10ug/ml Insulin; Intermediate Media is DMEM/F12, 5% Horse Serum, 0.5mg/ml Hydrocortisone, 100ng/ml Cholera Toxin, and 10ug/ml Insulin; and Minimal Media is DMEM/F12 and 5% Horse Serum. Mouse cell lines were grown DMEM at 10%FBS plus 1X GlutaMAX (ThermoFisher #35050061).

3.5.4 Western Blotting

Cells were lysed with RIPA buffer (25mM Tri-HCl, ph 7.5, 150nM NaCl, 0.1% SDS, 1% Sodium deoxycholate, 10% Triton-X, 5mM EDTA, pH 8.0 for 30 minutes on ice and cell debris was pelleted and supernatant was collected and BCA protein quantification was used to obtain protein concentrations.

3.5.5 RNAi Screening and Scoring

1000 cells/well were reverse transfected in quadruplicate with 0.05µl/well of RNAiMax and 5ng/well of each esiRNA, 72 hours after transfection plates were fixed with 3% PFA, and permeabilized with 0.5% TritonX. Hoechst 33342 Solution (Themo #62249) was added at a final concentration of 4µg/mL and incubated at 37°C for 30 minutes.

Nuclei were counted using a Thermo CellInsight microscope. Cell counts were normalized to a negative control non-targeting targeting esiRNA included in each plate and a Student's t-test was used to determine a p-value of significance by comparing normalized counts for each esiRNA in KRAS versus eGFP cells. Genetic interactions scores were based on Log_{10}(p-value) and signed to reflect synthetic sickness (negative) and enhancement (positive). P-values were used to estimate false discovery rates (FDR) using Benjamin-Hochberg method [81]. For esiRNA studies non-targeting esiRNA targeting eGFP (Sigma, #EHUEGFP). For siRNA studies, siBRCA1 is an ON-TARGET SMARTpool (Dharmacon, #L-003461-00-0005) and siNT is ON-TARGET NT4 (Dharmacon #D001810-04-05).

For the combinatorial E-MAP screen 5ng of each of 96 esiRNAs ("array") was plated in quadruplicate into 384 well plates to which was added a second constant "query" esiRNA (5ng) using a Mantis Liquid Handler to all wells along with 10 µl of RNAiMax to prepare reverse transfection mix, cells were plated and allowed to grow for 72 hours. At end point plates were processed as above for cell count. Counts were normalized to the median of each plate and Z-scored. Four replicates were averaged to obtain a mean Z-score per esiRNA combination.

The cellular context score of each gene was defined as the variance of KRAS genetic interaction scores across three conditions. The genetic context score was based on the number of significant genetic suppressors (E-MAP interaction score Z>2) identified for

each gene. The product of these two metrics was used to define the ranking and then Z-normalized for visualization.

3.5.6 Drug Screening

1000 cells/well in a 384 well plate were seeded and exposed to the drug library the next day. Drug plates were prepared by diluting stock drug into a 4 replicate 4-point dilutions series (500, 250, 50, 5ng/mL). Each dose was added in 4 replicates using a Caliper Zephyr liquid handler. Cells were allowed to grow for 72 hours before nuclei counting. Cell counts were normalized to DMSO control wells and area under the dose-response curve (AUC) was calculated as the sum of proliferation values over all 4 concentrations.

3.5.7 γH2AX Immunofluorescence

Cells were plated into 6-well plates containing coverslips and allowed to grow overnight prior to treatment with talazoparib. For washout, cells were washed twice with PBS, and allowed to grow in fresh media without talazoparib. Cells were fixed using 4% PFA for 10 minutes at room temperature, permeabilized using 0.3% Triton-X in DPBS, and blocked with 3% BSA in PBS. Cells were incubated with the primary antibody overnight at 4 C (Anti-Histone γ-H2AX, #07-627 clone PC130, Millipore Sigma 1:1000) and the secondary antibody (Goat anti-Mouse Alexa Fluor 647 Polyclonal, Thermo Fisher) for 1 hour at room temperature. Following washes with PBS and water, coverslips were

mounted using Prolong Antifade containing DAPI (P36931). Foci were quantified using ImageJ plugin Foci Counter (The Bioimaging Center, University of Konstanz).

3.5.8 Drug response curves and colony formation assays

For IC50 determination, 500 cells were seeded into 384-well plates overnight, then exposed to drugs and allowed to proliferate for 96 hours. Cells were quantified using nuclei counting and compared to cell counts with DMSO treatment. Curves were fit and IC50 determined using Graphad Prism nonlinear regression analysis. For colony formation assays, 500 cells were plated onto 12-well plates overnight before drug addition. Media and drugs were changed every 72 hours. Cells were fixed and stained with 1% crystal violet in 20% methanol. Plates were washed with water, dried and imaged using Epson V600 scanner.

3.6 Acknowledgments

The authors thank Alan Ashworth and Hayley Donnella for helpful discussions and assistance. This work was supported by National Cancer Institute grant nos. U01CA168370 (S.B.) and UC MEXUS Research grant DI-16-33 (A.A.K.)

3.7 Author Contributions

Conceptualization, A.K. and S.B.; Methodology, A.K.; Software and formal Analysis, A.K., SB; Investigation: A.K., H.H., X.Z., S.K., W.D.; Resources, S.B., F.M., A.B; Supervision and Project Administration: S.B.; Writing: A.K., S.B.

3.8 Main Figures

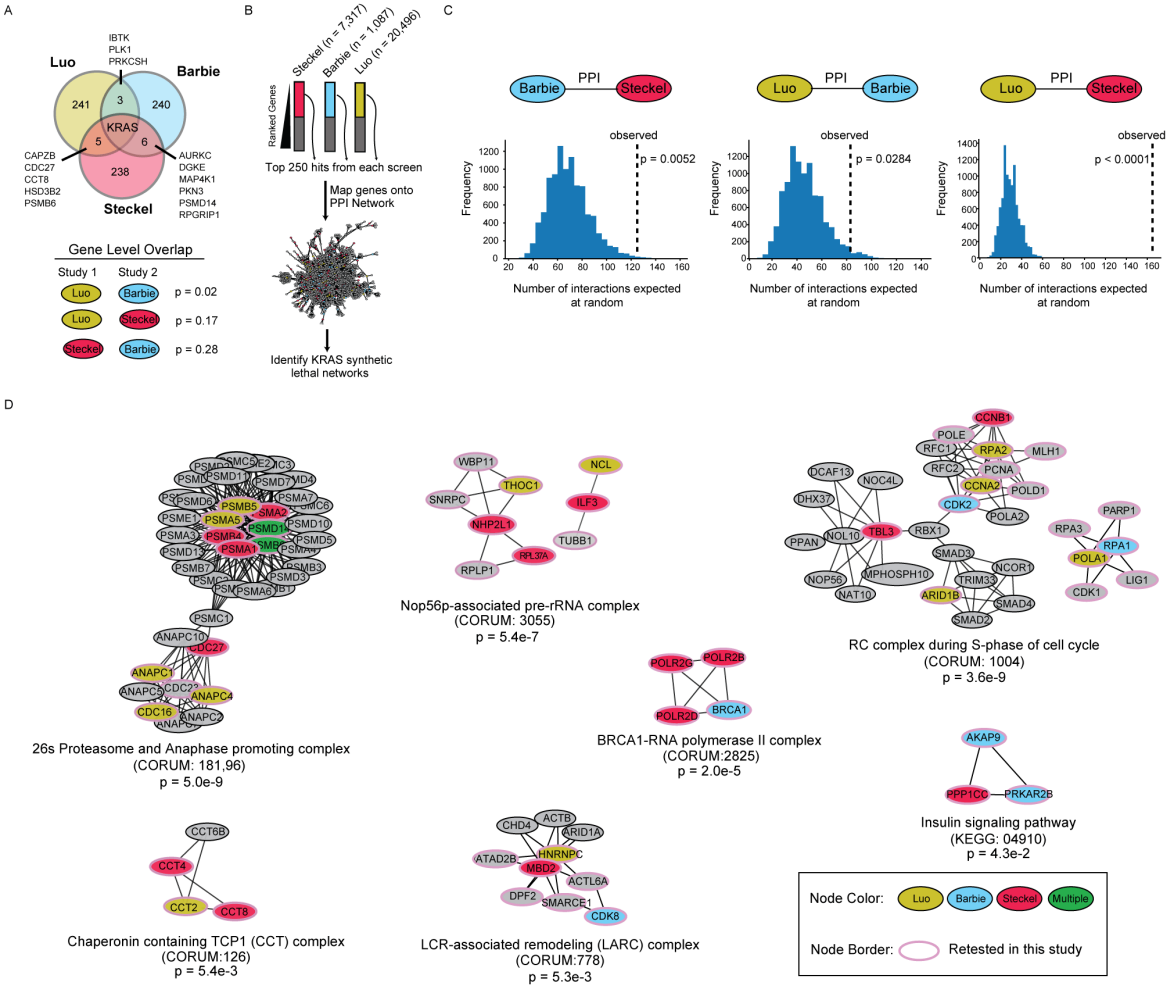

Figure 3.1 Meta-analysis of published studies identifies common KRAS synthetic lethal networks.

(A) Gene overlap between the top 250 hit genes reported from three published KRAS synthetic lethal studies, Luo et al, Barbie et al., and Steckel et al. [17,19,20]. P-values based on two-tailed hypergeometric test calculated between pairwise comparisons taking into account all tested genes per study. (B) Data integration strategy for mapping top 250 KRAS synthetic lethal reported from each study onto a protein-protein interaction network composed on interactions from HumanNet and CORUM protein complexes. The number of genes that were tested in each study, n. (C) Comparison of the number of interactions observed in the protein-protein interaction (PPI) network spanning between hits reported in the two indicated studies versus the number of similar interactions observed between random genes. Histogram represents results from 10,000 simulations conducted from randomly picking 250 genes that were tested in each respective study and the p-value represents the fraction of simulations where the same or more interactions than the actual observed number were obtained. (D) The PPI network was limited to interactions where at least one of the proteins was identified in previous studies and then subjected to network clustering to identify densely connected components using MCODE. Individual subnetworks were filtered to those which contained genes from multiple studies and grouped based on gene function into 7 clusters. The set of genes identified in each subnetwork was assessed for overlap with the CORUM or KEGG complex or pathway listed using a two-tailed hypergeometric test.

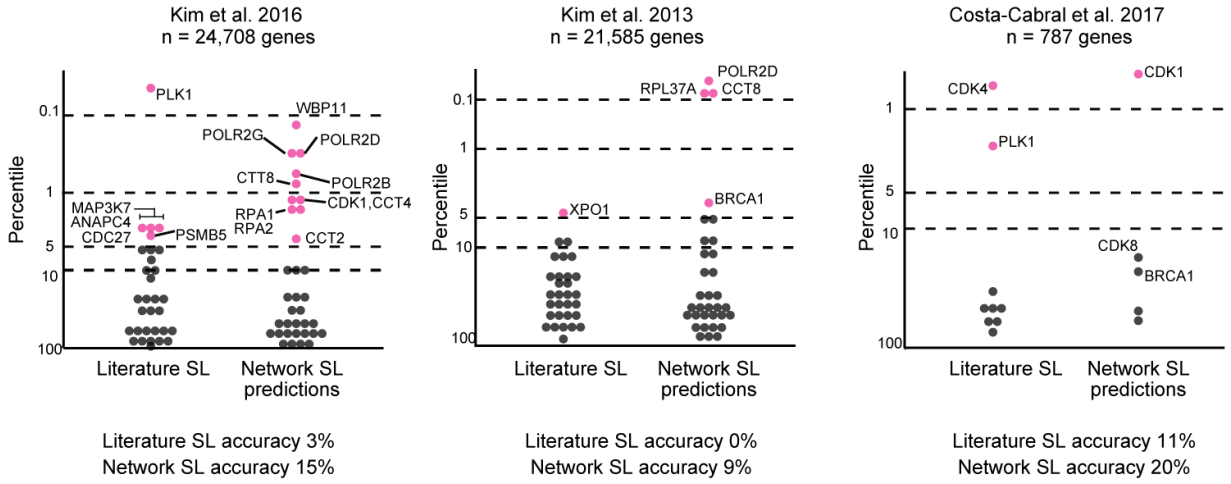

Figure 3.2 Comparison of genes in KRAS synthetic lethal networks and previously published KRAS synthetic lethal genes in held-out studies.

105 predicted KRAS synthetic lethal network genes and 26 previously published KRAS synthetic lethals were evaluated using data from Kim et al 2013, Kim et al 2016, and Costa-Cabral et al. [16,46,47]. Genes in each study were ranked into percentiles based on the difference in proliferation after knockdown in KRAS-mutant versus wild-type cell lines. The lower the percentile the more evidence for KRAS specific synthetic lethality. Accuracy calculated as the number of genes in the top 5% (pink dots) out of all the tested genes per category. The number of genes tested in each study, n.

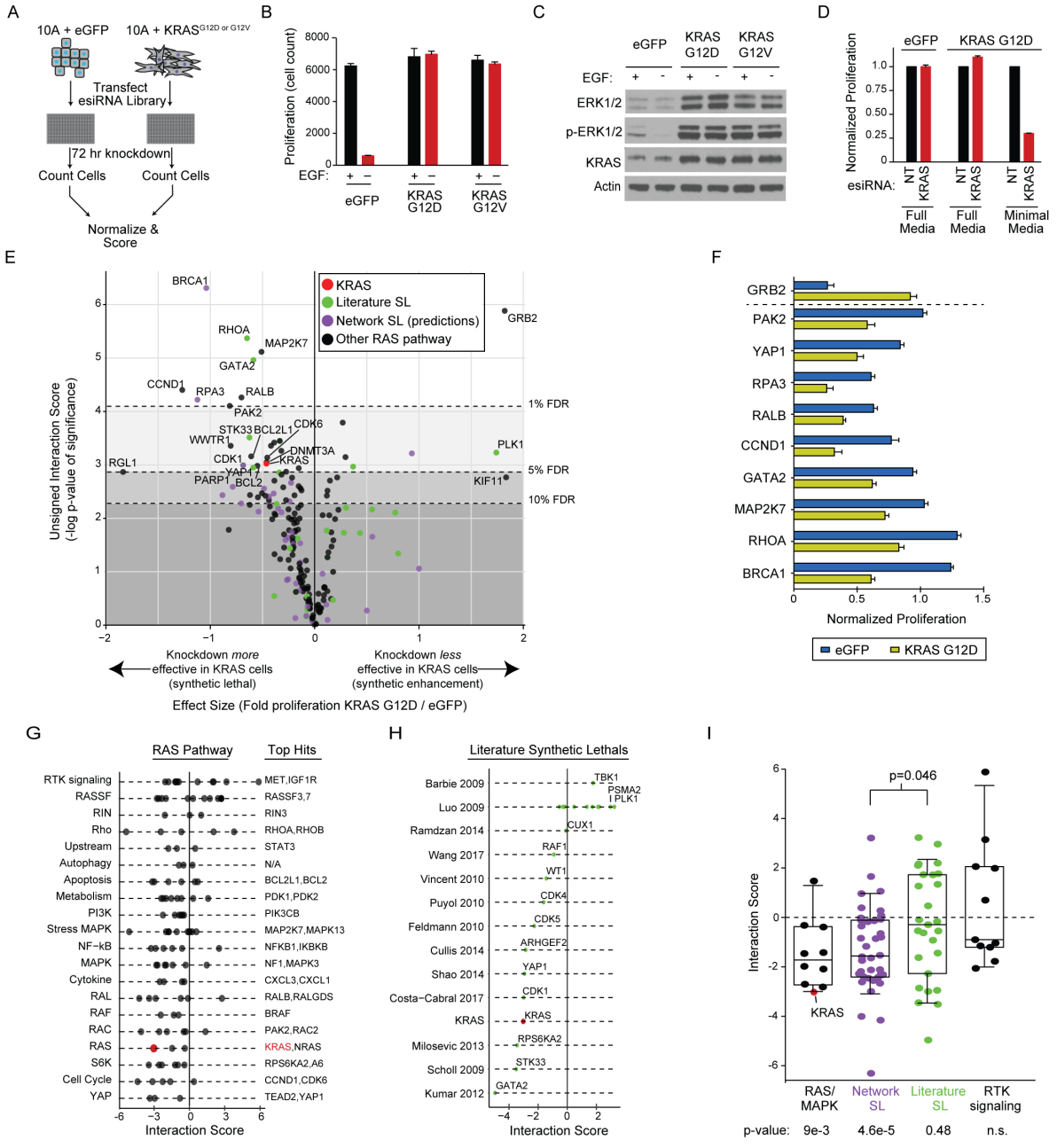
A
10A + eGFP
10A + KRASG12D or G12V
Transfect esiRNA Library
72 hr knockdown
Count Cells
Count Cells
Normalize & Score
B
Proliferation (cell count)
EGF:
eGFP
KRAS G12D
KRAS G12V
C
eGFP
KRAS G12D
KRAS G12V
EGF:
ERK1/2
p-ERK1/2
KRAS
Actin
D
eGFP
KRAS G12D
Normalized Proliferation
esiRNA:
NT
KRAS
Full Media
Minimal Media
E
KRAS
Literature SL
Network SL (predictions)
Other RAS pathway
1% FDR
5% FDR
10% FDR
Unsigned Interaction Score (-log p-value of significance)
Knockdown more effective in KRAS cells (synthetic lethal)
Knockdown less effective in KRAS cells (synthetic enhancement)
Effect Size (Fold proliferation KRAS G12D / eGFP)
F
Normalized Proliferation
eGFP
KRAS G12D
G
RAS Pathway
Top Hits
Interaction Score
H
Literature Synthetic Lethals
Interaction Score
I
p=0.046
Interaction Score
RAS/ MAPK
Network SL
Literature SL
RTK signaling
p-value:
9e-3
4.6e-5
0.48
n.s.

Figure 3.3 A new isogenic cell line screen validates KRAS synthetic lethal network genes.

(A) Overview of approach. MCF10A cells stably expressing eGFP or a mutant KRAS construct were reverse transfected with esiRNAs targeting specific genes. After 72 hours, relative proliferation was compared between eGFP and KRAS mutant cells to score genetic interactions. (B) Proliferation based on cell count of uniformly plated MCF10A cells expressing eGFP, KRAS G12V or G12D grown in the presence or absence of 20ng/ml EGF for 72 hours. (C) Immunoblot of lysates from isogenic cells grown in the presence or absence of 20ng/ml EGF for 24 hours. (D) Proliferation of eGFP or KRAS G12D cells grown in the indicated media conditions after non-targeting (NT) or KRAS knockdown for 72 hours, normalized to NT control. (E) Volcano plot of KRAS G12D screen reflecting the magnitude of change in proliferation after gene knockdown in KRAS G12D versus eGFP expressing lines versus the significance of this effect calculated among replicates. Dotted lines represent the indicated false discovery rate (FDR) cutoffs. (F) Relative proliferation of knockdown of listed genes in eGFP or KRAS G12D cells compared to non-targeting control in each respective cell line. Genes selected based on genetic interactions with <1% FDR. (G) Signed genetic interaction scores for genes in the broader RAS pathway grouped into functional categories. The most negative scoring genes in each category are listed. (H) Signed genetic interaction score of retested literature curated KRAS synthetic lethal genes and their source. Only a subset of genes from Luo et al. are indicated for clarity. (I) Comparison of genetic interaction scores for genes involved in the RAS or MAPK pathway (RAS/MAPK), RTK signaling, KRAS synthetic lethal genes from the literature (green), or predicted synthetic lethal network genes (purple). P-values based on comparison against a median interaction score of zero (bottom) and between groups (above), both by two-tailed Student's t-test. Boxes represent the median, hinges span 25-75th percentile and whiskers span 10-90th percentile. Error bars are s.d.

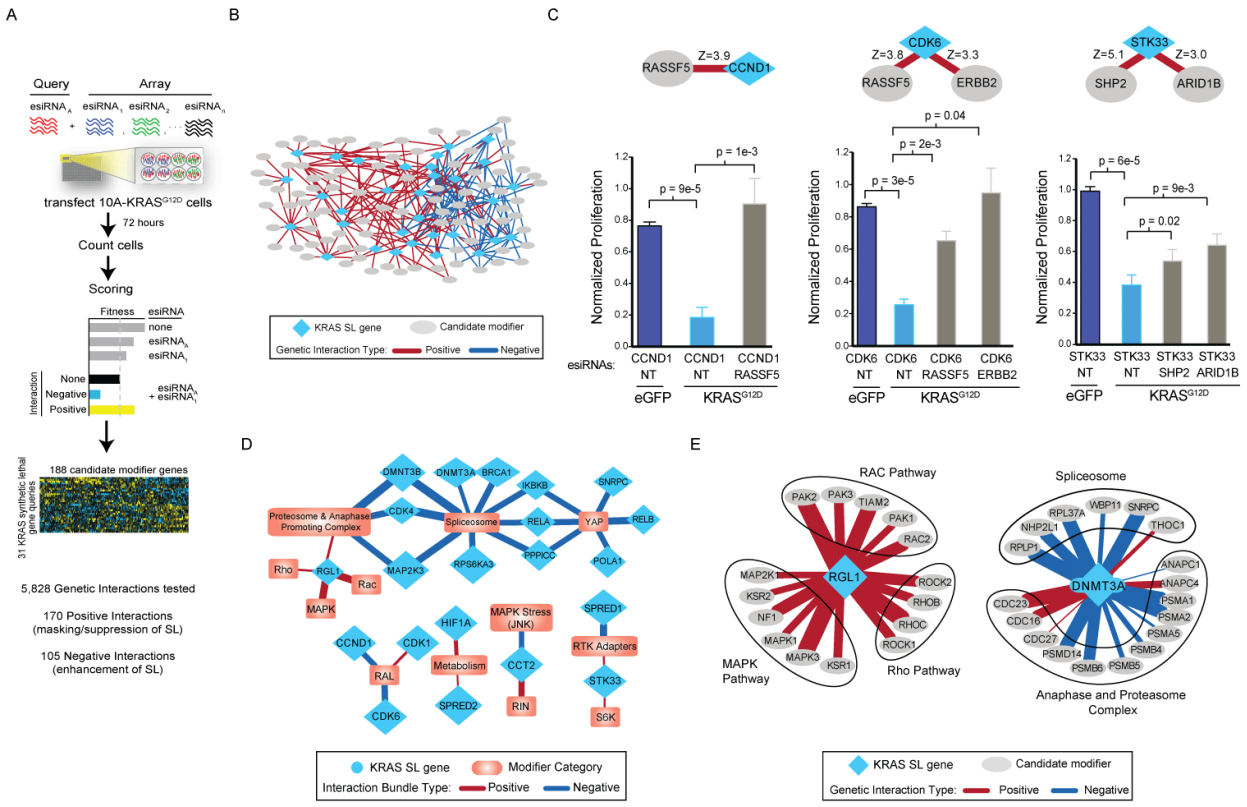

Figure 3.4 A genetic interaction map identifies KRAS synthetic lethal suppressors.

(A) Overview of approach to generate an epistatic mini-array profile (E-MAP) using combinatorial RNAi to measure 5,828 pairwise genetic interactions in MCF10A KRAS G12D cells. esiRNAs targeting a set of genes are arrayed in a pairwise fashion (in quadruplicate) in tissue culture plates. Reverse transfection is then performed, and the resulting fitness defects are observed using high-content imaging. Raw data is normalized and scored (see Methods) (B) Overview of genetic interaction map for 30 KRAS synthetic lethal genes and candidate modifiers. Interactions scoring >2 or <-2 are shown. (C) Relative proliferation of knockdown of three KRAS synthetic lethals identified or confirmed in this study, CCND1, CDK6 and STK33, in eGFP or KRAS G12D MCF10A cells alone and in combination with their top positive interaction partners. Proliferation normalized to mock. P-values based on a two-sided t-test, error bars s.d. (D) Categorical annotations for groups of genes displaying significantly strong genetic interactions with synthetic lethal query genes with p<0.01 (see Methods). (E) Genetic interaction partners involving two KRAS synthetic lethal genes identified in this study, RGL1 and DNMT3A, and associated pathways enriched for genetic interactions. Edge thickness is proportional to interaction score.

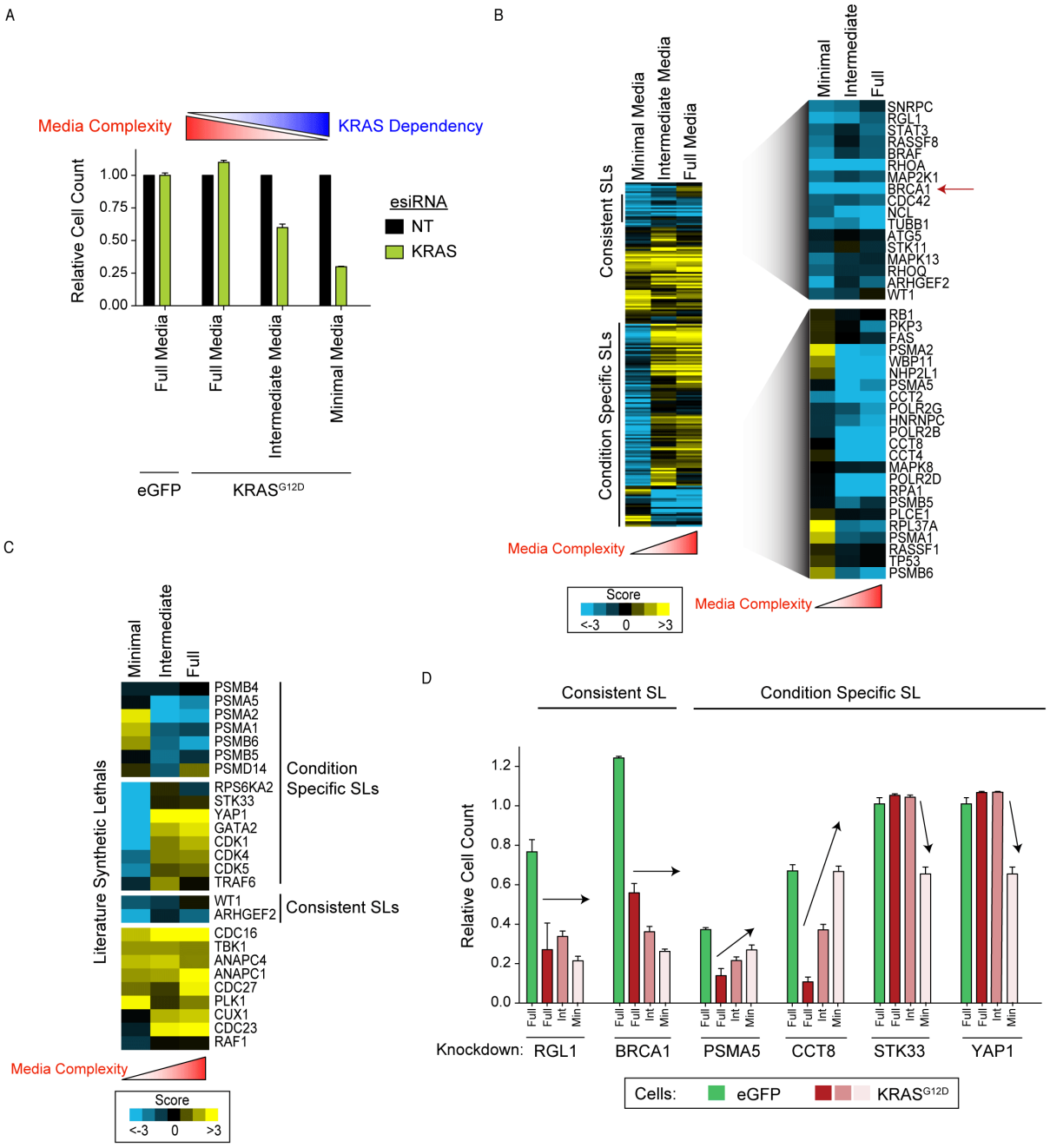

Figure 3.5 Dependency on synthetic lethal genes vary based on cellular conditions.

(A) Knockdown of KRAS or non-targeting (NT) in MCF10A eGFP or KRAS G12D cells in the indicated media condition for 72 hours. Proliferation measured relative to NT. (B) Heatmap of genetic interaction scores for KRAS G12D cells grown in full, intermediate or minimal media conditions compared to eGFP cells. Highlighted gene sets show consistent or condition specific synthetic lethality across conditions. Red arrow highlights BRCA1 as a consistent KRAS synthetic lethal. (C) Heatmap of genetic interaction scores for previously published KRAS synthetic lethals across different growth conditions. (D) Proliferation of cells grown in the indicated conditions harboring knockdown of indicated genes normalized to NT transfection control. Full = full media, Int = intermediate media, Min = minimal media. Error bars are s.d.

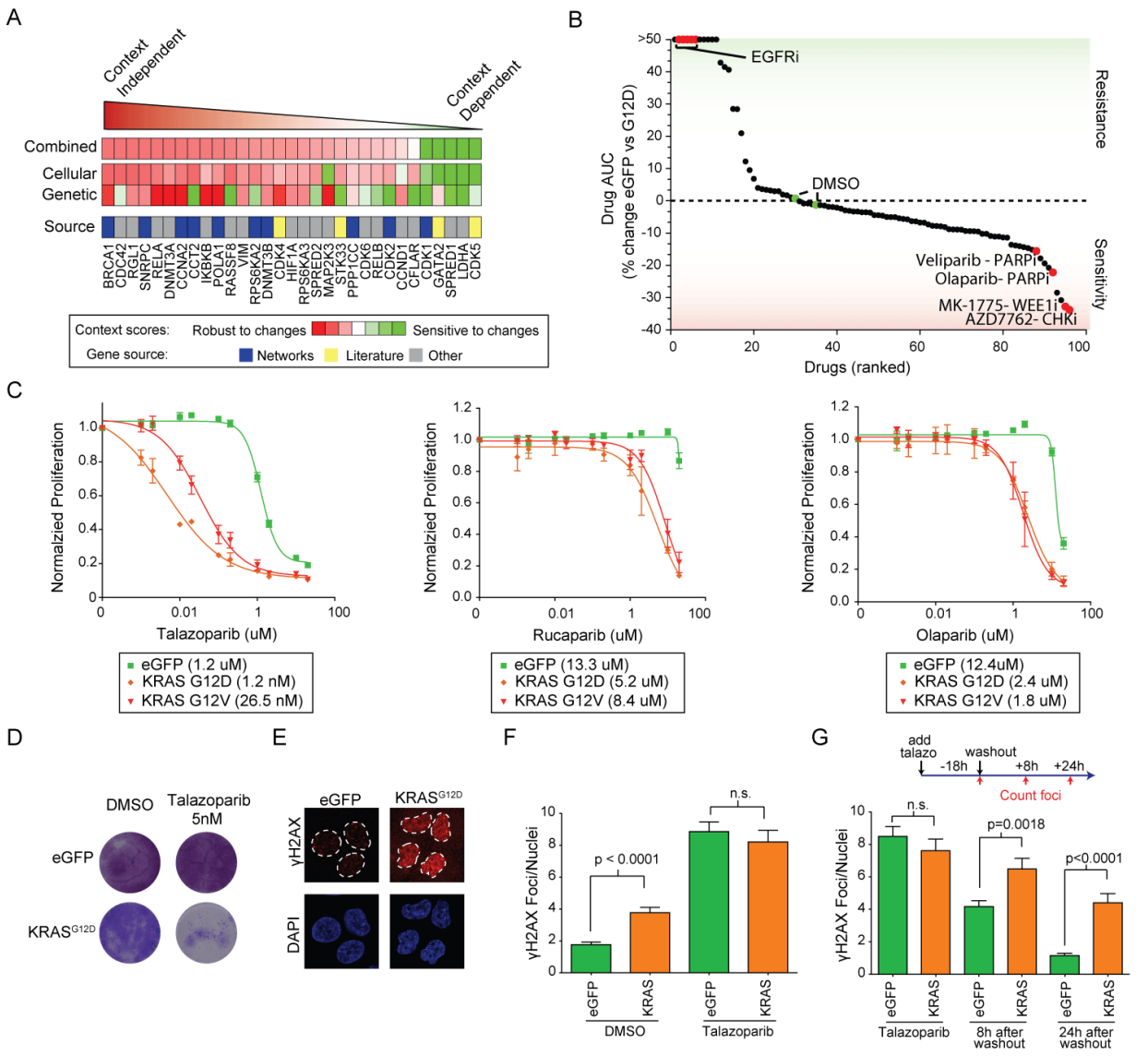

Figure 3.6 PARP inhibitors are more effective in oncogenic KRAS expressing cells.

(A) Ranking of candidate KRAS synthetic lethal genes based on integration of genetic and cellular perturbation screens. Genes were selected for analysis based on evidence of synthetic lethality in MCF10A KRAS cells grown in minimal media. The conceptual source of each gene is listed. (B) Drug screen of 91 clinically relevant compounds ranked by sensitivity based on difference in the drug area under the curve (AUC) between eGFP and KRAS G12D cells. DMSO and EGFR inhibitors indicated as controls for no effect and KRAS induced drug resistance, respectively. (C) Relative proliferation of control eGFP, KRAS G12D or G12V expressing MCF10A lines after treatment with PARP inhibitors talazoparib, rucaparib or olaparib for 72 hours. IC_{50} values are shown. (D) Long-term clonogenic growth of MCF10A KRAS G12D and eGFP cells treated with DMSO or talazoparib for two weeks. (E) γH2AX immunofluorescence in eGFP or G12D expressing cells, red. Nuclei outlines in dotted lines based on DAPI staining. (F) Quantification of γH2AX foci in the indicated cell lines treated with DMSO or with 500nM of talazoparib for 18 hours. (G) Treatment of the indicated cells with 500nM talazoparib for 18 hours then washed out. γH2AX foci quantified before, 8 and 24 hours after washout. Error bars, s.d. except E and F which are s.e.m. Not significant, n.s.

3.9 Supplementary Figures

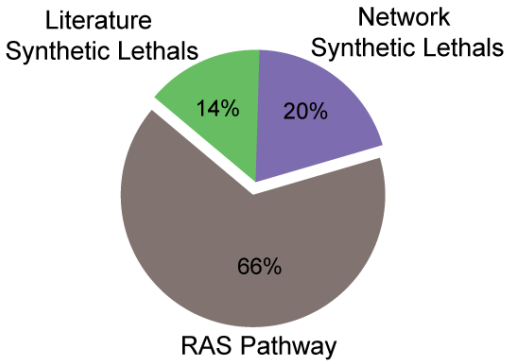

Supplementary Figure 3.1S: Distribution of 196 genes tested in esiRNA screen. Individual genes are listed in Supplementary Table 4.

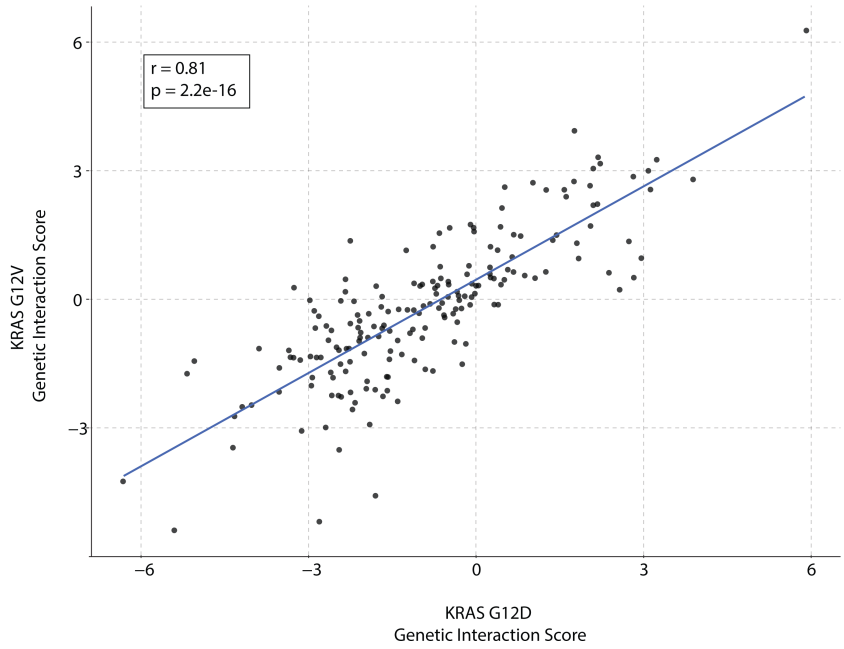

Supplementary Figure 3.2S: Comparison of KRAS G12V and G12D screens.

Isogenic KRAS G12V and KRAS G12D expressing MCF10A lines were screened using the same esiRNA library and scores for genes compared. P-value of Pearson's correlation (r) is shown.

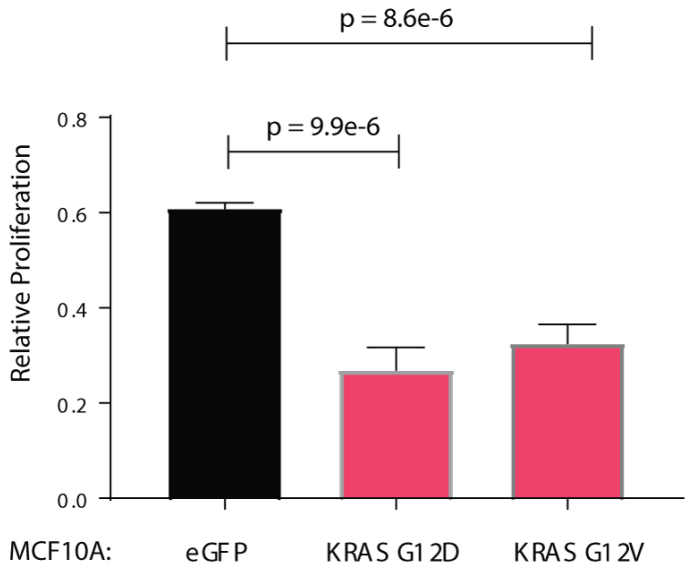

Supplementary Figure 3.3S: siRNA mediated validation of BRCA1 dependency in mutant KRAS cells. The indicated MCF10A isogenic cell lines were transfected with BRCA1 siRNA and proliferation measured over 72 hours. Data are proliferation relative to control non-targeting knockdown. P-values based on two-sided t-test. Error bars are s.d.

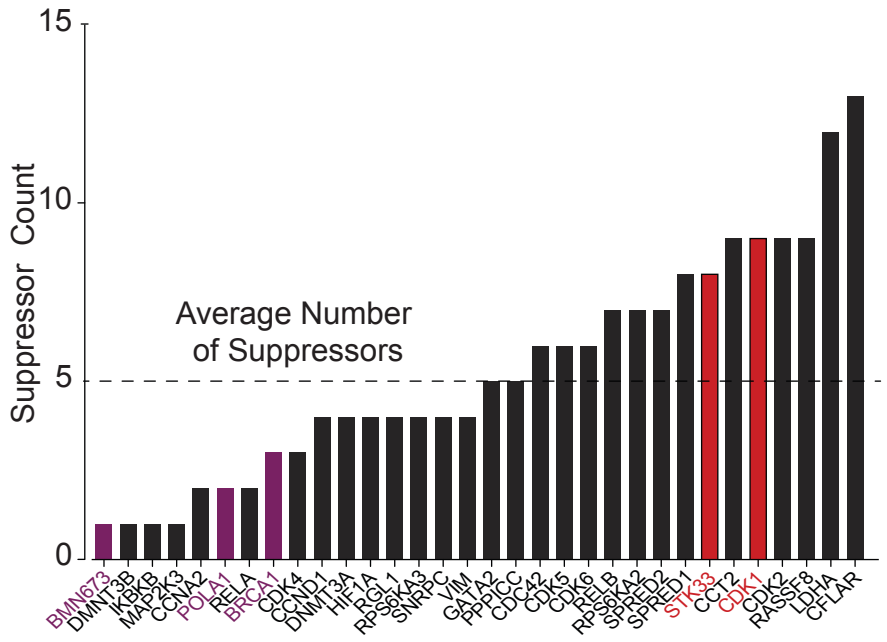

Supplementary Figure 3.4S: Suppressors of synthetic lethal genes. Histogram of the number of suppressor genes identified for KRAS synthetic lethal genes and talazoparib. Suppressors defined as genes with a *Z*-score > 2. Purple gene highlight network genes from the cell cycle/replication cluster, red genes highlight two published KRAS synthetic lethal genes with suppressor counts greater than average.

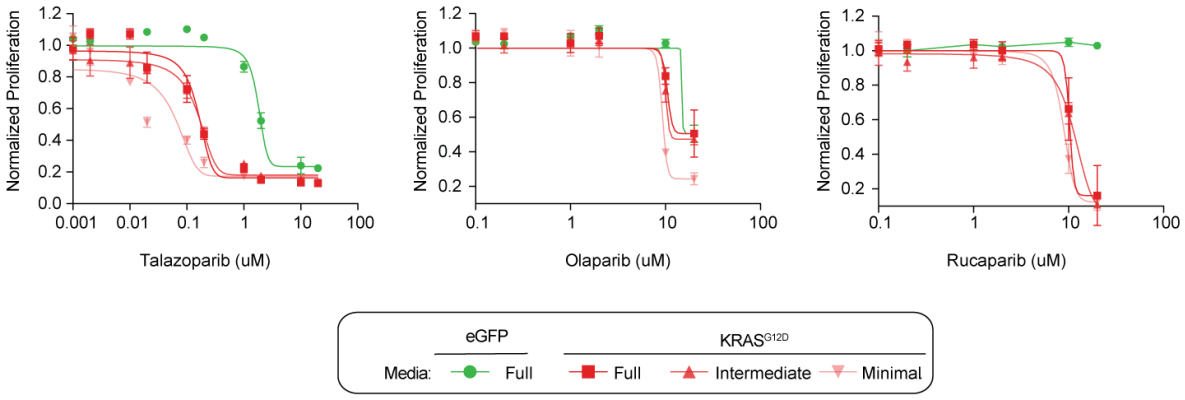

Supplementary Figure 3.5S: PARP inhibitor sensitivity is independent of media conditions. Relative proliferation of control eGFP and KRAS G12D MCF10A lines after treatment with PARP inhibitors talazoparib, rucaparib or olaparib for 96 hours in full, intermediate or minimal media conditions. Error bars, s.d.

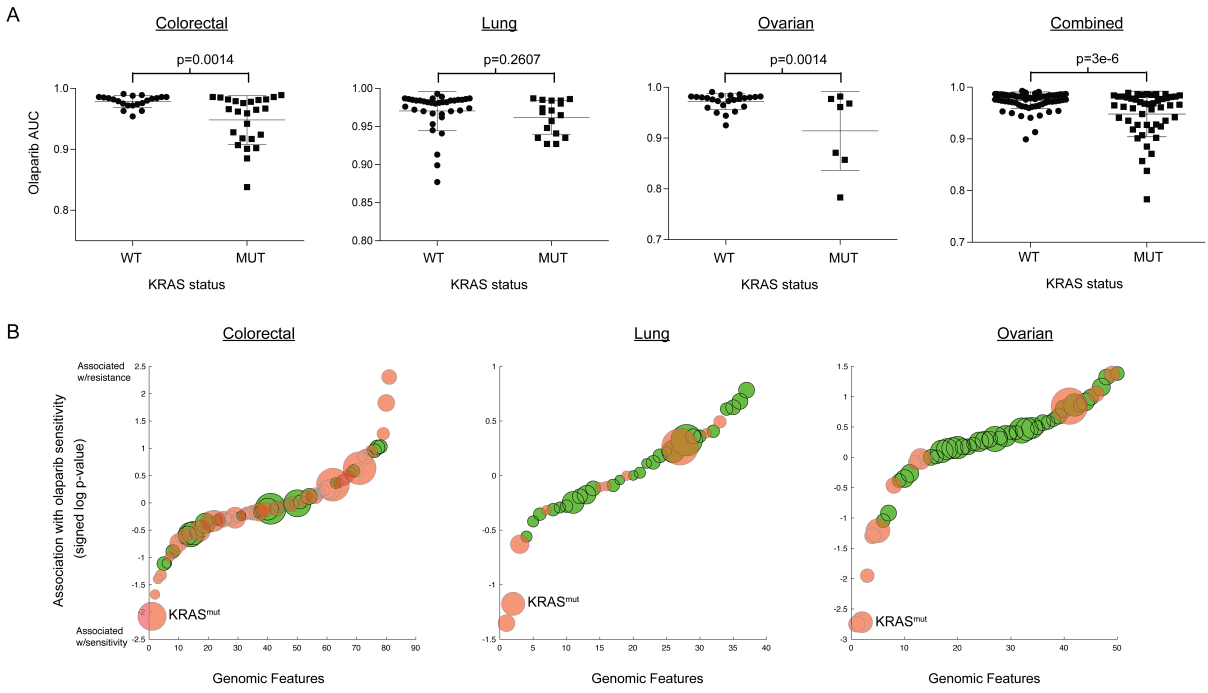

Supplementary Figure 3.6S: Olaparib drug response analysis in cancer cell lines collections. (A) Cell lines from the three different tumor types that harbor >5 KRAS mutant and >5 wild-type cell lines were analyzed with respect to olaparaib sensitivity in the genomics of drug sensitivity database (GDSC) [37]. Responses were compared based on drug area under the dose response curve (AUC) analysis [37] with lower values indicating more drug sensitivity. Shown are responses for each tumor type individually as well as all three combined. The number of cell lines in each category are shown. P-values based on a two-sided t-test. (B) Associations of genomic features with olaparib sensitivity downloaded from the GDSC database. P-values of association were converted into a signed score by taking the log of the p-value and adding a sign to indicate association with sensitivity (negative values) and association with resistance (positive values). Mutation based features in red and copy-number based features in green.

Chapter 4: Exploration of PARP inhibitors for KRAS mutant Non-Small Cell Lung Cancer

4.1 Abstract

PARP inhibitors are currently approved for BRCA mutant ovarian and breast cancers; however, there is interest cancers with DNA repair deficiencies (BRCAness) that may also benefit from PARP inhibitors. Recent studies have linked oncogenic RAS with increased DNA damage that may leave cells vulnerable to DNA repair inhibition. Similarly, work from my research has uncovered a DNA repair dependency in a MCF10A KRAS isogenic model; here I seek to characterize the response of KRAS mutant lung cancer cells to PARP inhibitors. I compare both traditional IC50 metrics and Growth Rate inhibition metric (GR50) to correct for differences in growth rates. My findings highlight heterogeneous response to both short term and long-term exposure to PARP inhibitor. Gene Set Enrichment Analysis (GSEA) of resistant and sensitive cell lines revealed molecular pathways associated with response. These findings highlight the complexity of developing therapeutic strategies and highlight the need for more a systematic interrogation of factors that affect PARP inhibitor sensitivity in KRAS mutant cell lines.

4.1 Introduction

Genome instability and telomere maintenance is hallmark of cancer and has been an area of great interest for therapeutic interventions[82]. Cancer cells depend on maintaining their genomes and therefore inhibiting DNA repair pathways was an early method of treating cancer (i.e. chemotherapy). Additionally, small molecule inhibitors have also been developed to target DNA repair kinases and mediators like CHK1, PARP1 and RAD51[83]. PARP inhibitors are currently used in the clinic to target BRCA1 mutant cancer, and an open area of research is to determine if PARP inhibitors can be used in cancers which have impaired DNA repair through non-BRCA1 mutant mechanism, a phenomenon known as “BRCAness”[54].

DNA damage repair defects and increased dependencies in DNA repair has been linked to oncogenic KRAS. For example, Oncogenic HRAS has been shown to drive the formation of DNA-RNA hybrids known as R-loops which causes DNA damage through stalling of replication forks[78]. When stalled replication forks collapse it forms a double stranded break that requires RAD51 for repair[53]. Mutant KRAS has been linked to inhibition of DNA repair through wild type HRAS and NRAS repressing CHK1 signaling[84]. Findings from my research have uncovered a DNA repair dependency in KRAS mutant isogenic MCF10a cells and demonstrated sensitivity to both genetic knockdown and chemical inhibition of PARP, BRCA1 and other DNA repair genes. An open area of research remains to determine if targeting these DNA repair dependencies in KRAS mutant cancers is a viable therapeutic strategy.

In this study we characterize the response of PARP inhibitors to a panel of KRAS mutant NSCLC cell lines. Due to the heterogeneity in growth rates we adopt a growth rate (GR) drug response metric and show that there is modest agreement between GR and IC50 metrics[85]. I leverage publicly available gene expression profiles from the Genomic of Drug Sensitivity portal for the cell lines tested in this study and identify pathways associated with response[37]. We identify a set of signatures linked to response and propose a model where KRAS dependent cells repress DNA repair, which leaves them vulnerable to PARP inhibition.

4.2 Results

4.2.1 Characterization of PARP inhibitor response across a panel of KRAS mutant NSCLC cell lines.

To test the efficacy of PARP inhibitor in KRAS mutant cancer we tested three inhibitors olaparib, rucaparib, and talazoparib on a panel of RAS mutant NSCLC cell lines (Figure 4.1A). A major limitation of the traditional sensitivity metric is that it is confounded by differences in growth rates. Data from recent study show that IC_{50} metrics are highly influenced by growth rates and propose the use of a GR_{50} (Concentration to inhibit 50% of the growth rate) metric account for growth rate of cells[85]. After 96 hours of drug exposure we fixed and counted cells (see Methods) and calculated GR_{50} and IC_{50} values for each cell line. My data shows variable response to all three inhibitors (Figure

4.2 B-E), and so to obtain one summary response metric I derived an aggregate rank for all three inhibitors by averaging rank in response per cell line across inhibitors. The mechanism of action for talazoparib is unique among the three drugs due to its ability to trap PARP onto the DNA and further increased DNA damage in cells[69]. Therefore, I derived an individual rank for talazoaparib and non-trappers oalaparib, and rucaparib to see if there are differences between the two types of PARP inhibitors. The most sensitive cells to talazoparib were H1573, H1373, and H358 (Figure 4.1F), while H647, H358 and H2347 were the most sensitive to non-trapping PARP inhibitors (Figure 4.1G). H1373 was the second most sensitive to talazoparib, but it was the second most resistant cell line to non-trapping PARP inhibition (Figure 4.1F, G). This suggest that although the enzymatic activity of PARP is not required for this cell, that having bound PARP enzymes to DNA is lethal. Finally, A549 and H2122 were consistently the most resistant cell line across all the PARP inhibitors. The only outlier in this analysis was H460, which was sensitive by IC_{50} metrics but resistant by GR_{50} metrics therefore we dropped this cell line from downstream analyses. These results show that GR50 metrics can correct growth rates and assist in characterizing drug sensitivity across panels of cell with variable growth rates.

4.2.2. Long term exposure to PARP inhibitors

PARP inhibitors are more effective over multiple cell cycles due to more opportunities to inhibit DNA repair and synthesis during S-phase, therefore to characterize PARP sensitivity we obtained drug sensitivity metrics over the course of 14-18 days. We

initially seeded 100 cells per cell and changed growth media and added drug every 72 hours. Once DMSO condition treatments reached confluency we prepared each cell line for staining and image analysis. Consistent with short-term exposure we observed variable response in the long-term exposure to PARP inhibitors (Figure 4.2A). We calculated IC_{50} values by using an ImageJ plug (see Methods). I then asked if long term and short-term metrics correlated, I compared the ranks of IC_{50} and GR_{50} values with the rank of long-term survival. Interestingly only talazoparib IC_{50} and GR_{50} correlated significantly with the long-term IC_{50} values (Figure 4.2B), while neither olaparib's nor rucparib's short term metrics had no significant correlation to long term IC_{50} (Figure 4.2C, D). These findings highlight that both long term and short-term response to PARP inhibition is variable for non-trapping PARP inhibitors, but that talazoparib's long term and short-term IC_{50} metrics correlated significantly.

4.2.3 GSEA analysis reveals molecular signatures associated with PARP response.

With established sensitivity profiles for reach of our cell lines I then asked if these two subsets exhibit molecular profile which may nominate genes correlating with response. I obtained gene expression profiles from the Genomics of Drug Sensitivity (GDSC) portal and analyzed the top three responders and non-responders using classic GSEA against the Hallmarks and Oncogenic gene sets[37,86]. This revealed 16 Hallmark and 18 Oncogenic signatures with FDR values less than 15% and nominal p-values less than 0.05. We observed that PARP sensitive cell lines had down regulated DNA repair, UV

response Up, E2F Targets, and G2M Checkpoints while in resistant cells had up regulated these pathways (Figure 4.3A). The Singh Et al. KRAS dependency signature was up regulated in KRAS PARP sensitive cell line and vice versa in resistant cells (Figure 4.3B).

To gain a better insight to the specific genes which contributed to significance I investigated the leading-edge subset of genes. Hallmarks signature “DNA Damage” response was down regulated in PARP sensitive cell lines, and within the top 50 leading edge genes LIG1, RAD51, ERCC3, and RPA3 were down regulated (Figure 4-3C). It is likely that a subset of KRAS mutant cell line suppress these genes that leave cells vulnerable to further inhibition to DNA repair. RAD51 is a mediator of double stranded DNA repair and is required for BRCA1 to repair DNA[87], it is possible that homology directed repair is suppressed not via BRCA1, but RAD51 in this model. This proposes a model where “BRCAness” manifests through loss of RAD51 and thus PARP inhibition lethal in this state.

The Singh et al KRAS Dependency signature was also up regulated in PARP sensitive cell lines (Figure 4-3D). KRAS dependency has been reported to be inversely correlated with epithelial to mesenchymal transition (EMT)[88]. In other words, KRAS dependent cells display epithelial markers, whereas KRAS independent cell lines are often mesenchymal. Additionally, I observed that PARP sensitive cells up regulated the “KRAS Signaling up” signature. Take together our data suggest that PARP sensitivity is linked to KRAS dependency and a suppression of DNA repair pathways.

4.3 Discussion

PARP inhibitors are approved for BRCA1/2 mutant ovarian and breast cancers; however, and open area of research is to identify other DNA repair deficient tumors where PARP inhibitors could be effective. One approach is to identify non-BRCA1 mutant cells which have repressed DNA repair pathways which leave them vulnerable DNA repair inhibitors, and phenomena known as BRCAness[54].

Here I show that KRAS mutant lung cancer cells' response to PARP inhibition is heterogeneous by both traditional and growth rate drug sensitivity metrics. This also revealed that GR_{50} metrics can correct for large differences in growth rates and identify problematic cells which can confound validation studies. Interestingly only talazoparib's short term metrics correlated significantly with long term IC_{50} (Figure 4-2D), and overall the short term IC_{50} correlated better (r=0.95).

Leveraging public data sets I used the molecular profiles of cell lines tested here to query the pathways associated with response and resistance. GSEA analysis revealed EMT as a molecular signature associated with PARP inhibitor resistance. EMT has been linked to altering the degree of KRAS dependency in 2D cell culture[61]. Consistent with this observation, we observed the enrichment of "Signh et al KRAS dependency" signature in PARP inhibitor sensitive cell (Figure 4-3 D). We also observed that PARP inhibitor sensitive cells suppressed DNA repair signatures (Figure 4-2A), with RAD51 as

a leading-edge subset gene. This proposes a model where KRAS dependent cell lines have a compromised DNA damage repair pathway which be exploited with PARP inhibition. It remains unclear if KRAS dependency is altered *in vivo*, however 3D cell culture experiments in the context of KRAS inhibitors suggest that all cell line become KRAS dependent in 3D cell culture[89]. While, this may indeed play a major role in dictating sensitivity there may be other factor that were not present in our focused panel of cell lines. Future work will focus on systematically interrogating genes that modulate response to PARP inhibitors in the context of mutant KRAS.

4.4 Methods

4.4.1 Drug sensitivity profiling and Growth Rate metric calculations

For IC_{50} determination, 500 cells were seeded into 384-well plates overnight, then exposed to drugs and allowed to proliferate for 96 hours. For G_{50} determination a replicate plate was fixed before drug exposure to obtain at T_0 time point plate. Cells were quantified using nuclei counting and compared to cell counts with DMSO treatment. GR_{50} and IC_{50} metrics were calculated using the GR_{50} calculator (http://www.grcalculator.org)[90]. For colony formation assays, 100 cells were plated onto 24-well plates overnight before drug addition. Media and drugs were changed every 72 hours. Cells were fixed and stained with 1% crystal violet in 20% methanol. Plates were washed with water, dried and imaged using Epson V600 scanner. Cell were quantified using relative area (Imagej plugin ColonyArea[91]) to area of DMSO treatments, IC50 were calculated using GraphPad's nonlinear regression analysis.

4.4.2 Expression profiles and GSEA analysis of NSCLC responders

Processed and normalized gene expression profiles were downloaded from the Genomics of Drug Sensitive portal[37] and formatted to meet the requirements for classic GSEA. Classic GSEA was conducted on expression profiles, and permutations settings were set to 'gene set' for all analyses. Only signatures with FDR values less than 15% and adjusted p-values less than 0.05 were considered a significant and used for downstream analysis.

4.5 Figures

A

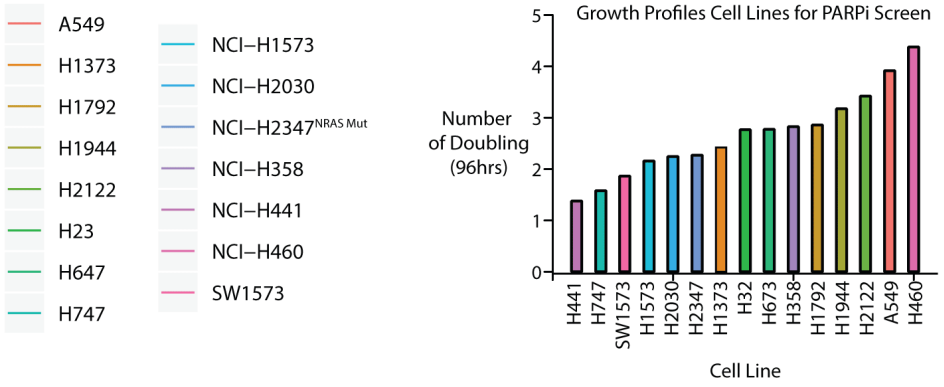

B

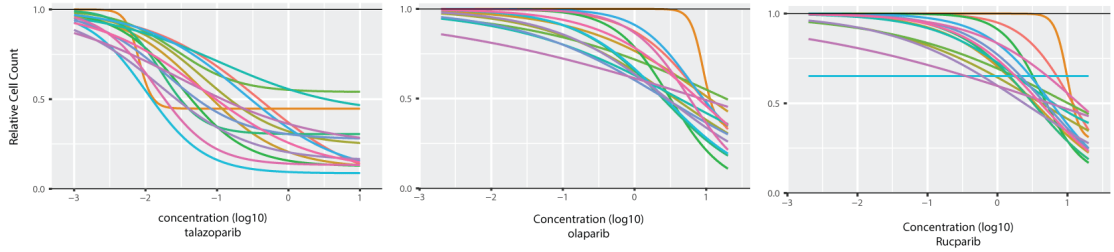

C

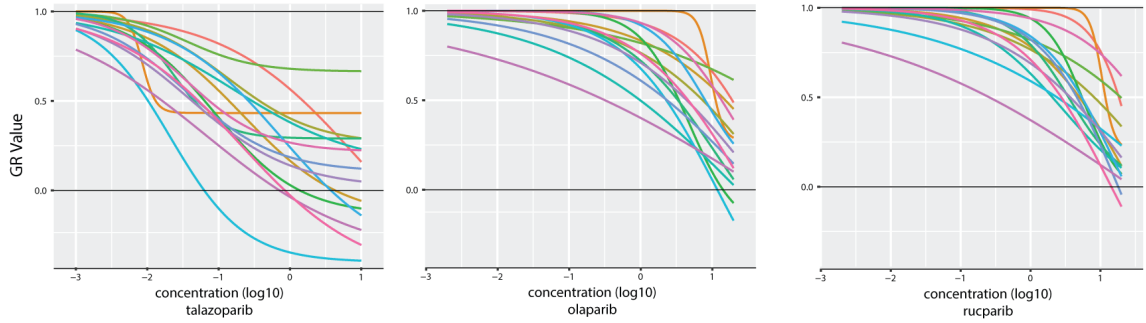

D

IC50 Values (uM)

Cell Line	Talazoparib	Olaparib	Rucaparib
H647	0.0306	2.47	3.23
NCI-H1573	0.0122	2.66	Inf
NCI-H2347	0.0521	2.7	4.76
NCI-H358	0.027	2.85	2.41
H23	0.0435	3.16	4.98
H1944	0.149	3.68	4.25
H747	3.34	4.19	6.32
NCI-H460	0.0185	5.87	14.4
SW1573	0.0958	7.69	4.13
NCI-H441	0.118	8.54	5.61
A549	0.388	8.95	11.9
NCI-H2030	0.294	9.1	5.9
H1792	0.0856	11.1	3.45
H1373	0.013	11.2	11.8
H2122	Inf	18.8	10.2

E

GR50 Values (uM)

Cell Line	Talazoparib	Olaparib	Rucaparib
NCI-H441	0.0163	0.321	0.256
H747	0.295	0.994	2.05
NCI-H1573	0.0103	2.3	2.39
NCI-H2347	0.0501	2.36	4.6
H647	0.0453	3.35	3.49
H23	0.0638	3.45	5.45
NCI-H358	0.0424	4.45	3.69
SW1573	0.0523	4.65	2.75
H1944	0.375	7.44	8.14
NCI-H2030	0.262	8.04	5.41
H1373	0.0131	11.2	11.8
NCI-H460	0.0741	13.6	33.4
H1792	0.14	15.4	4.99
A549	1.53	19.2	18.3
H2122	Inf	62.1	19.5

F

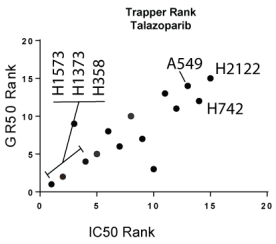

G

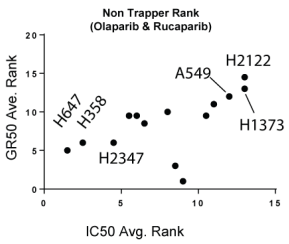

Figure 4.1 PARP inhibitors response across KRAS mutant NSCLC cell lines.

(A) List of RAS mutant Non-Small Cell Lung cancer cell lines used for short term PARP inhibitor screen and the number of divisions during the 96 hours of drug exposure (B) Conventional dose response profiles of KRAS mutant lung cancer cell lines for talazoparib, olaparib, and rucacparib. (C) Growth Rate metric response profile for RAS mutant cell lines across three PARP inhibitors. (D) IC_{50} (μM) table for PARP inhibitors. (E) GR_{50} metrics (μM) for PARP inhibitors. (F) Talazoparib (Trapper) IC_{50} versus GR_{50} ranks plot G) Non-trapping PARP inhibitors IC50 versus GR50 average ranks plot.

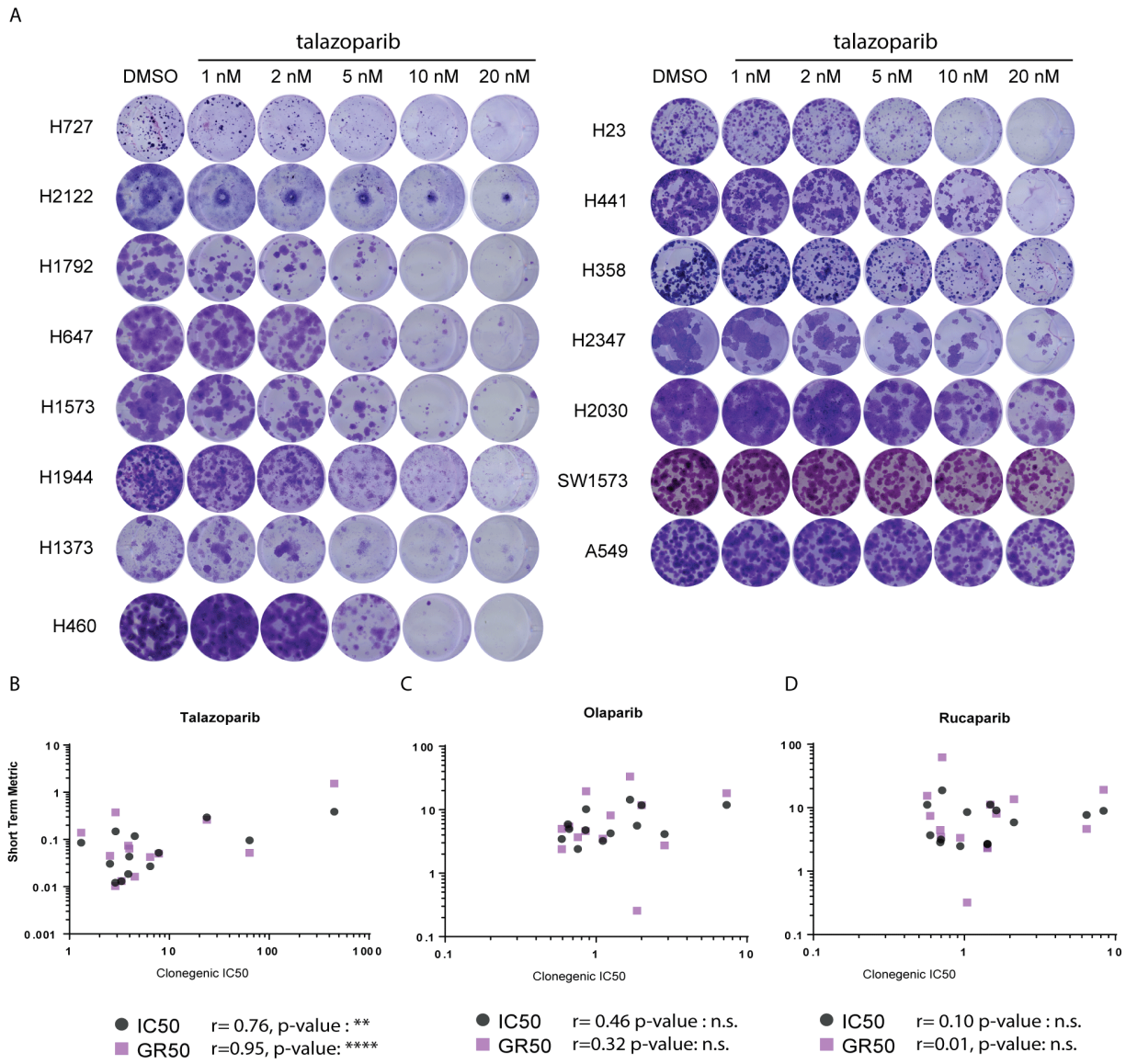

Figure 4.2 Clonegenic growth in presence of PARP inhibitor across NSCLC panel.

(A) Representative (quadruplicates) images of long-term drug exposure assays for talazoparib (B) IC_{50} values from clonegenic growth assays. (B) Correlation of talazoparib's short-term GR_{50} and IC_{50} values with clonegenic IC_{50} values. (C) Correlation of olaparib's short-term GR_{50} and IC_{50} values with clonegenic IC_{50} values. (B) Correlation of rucaparib's short-term GR50 and IC_{50} values with clonegenic IC_{50} values.

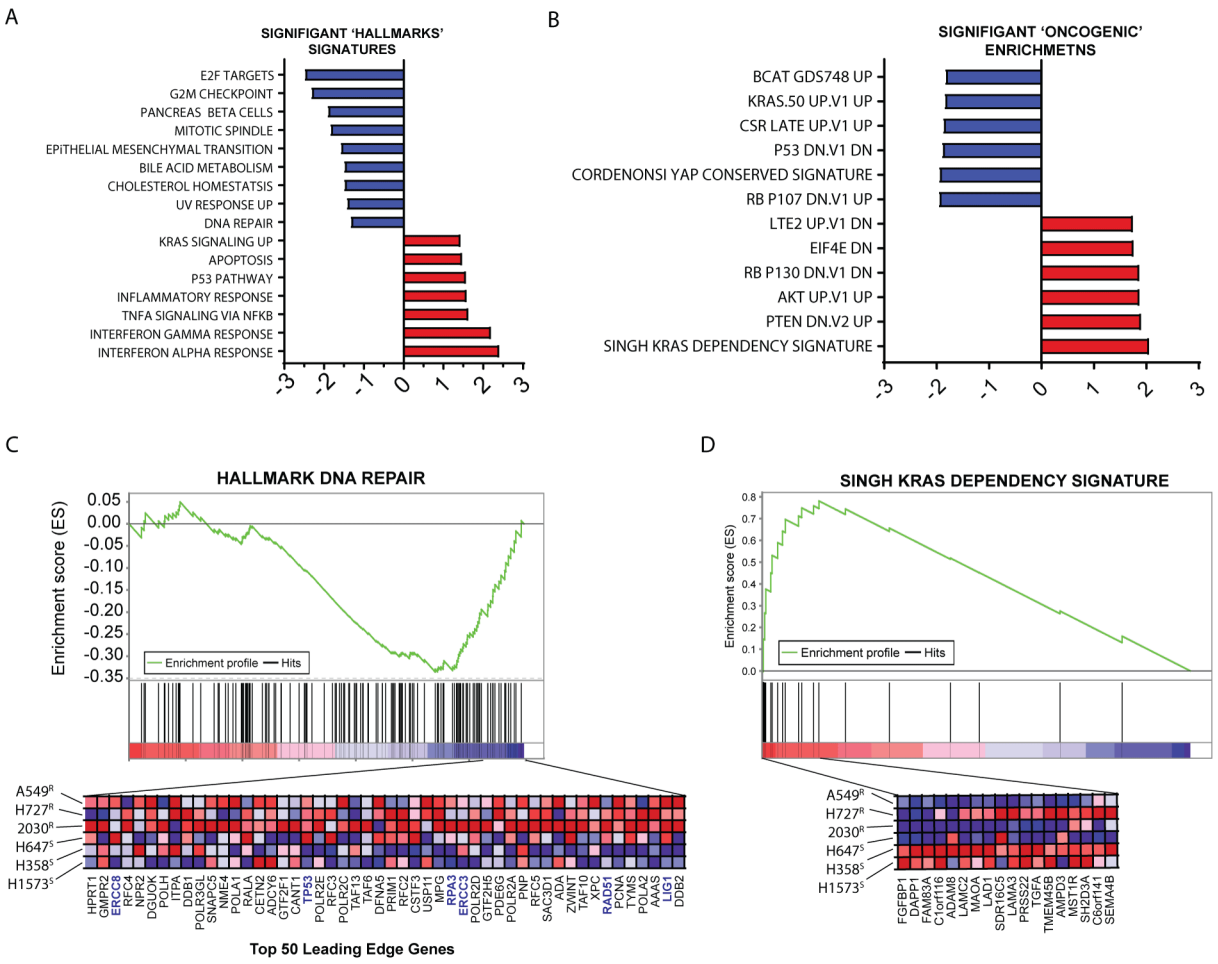

Figure 4.3 GSEA of PARP inhibitor sensitive and resistant cell lines.

(A) Bar plot of significantly enriched hallmark gene sets with FDR less than 15% and nom-p-values less than 0.05. (B) Bar plot of significantly enriched 'oncogenic signatures' sets with FDR less than 15% and nom-p-values less than 0.05 (C) Enrichment plot for Hallmarks DNA REPAIR gene set and the top 50 leading edge genes heatmap of sensitive and resistant cell lines. Blue text denotes DNA repair genes involved in repair of double stranded breaks. (D) Oncogenic signature's "Singh et al. KRAS Dependency" gene set and leading-edge subset heatmap.

Chapter 5: A KRAS 4a and 4b drug screen identifies isoform specific therapeutic opportunities for KRAS mutant cancers.

5.1 Abstract:

KRAS 4b is the most studied isoform of KRAS and therefore many studies have focused on this specific splice variant of KRAS. However, recent studies have revealed that both isoforms have unique properties that may have implications for caner. This study we set out to determine if alteration in ratios between 4a and 4b offer any therapeutic opportunities. Through CRISPR edited KRAS mutant lung and pancreatic cancer cell lines we show that cell which express more 4a are sensitive to MEK inhibitors. While cell lines that express more 4b are sensitive to Checkpoint kinase, mitotic, and Protein Kinase C inhibitors. These results highlight that the ration between 4a and 4b make cell vulnerable to different chemical agents and and sets forth a new avenue to explore to better target KRAS.

5.2 Introduction

KRAS has two splice variants: KRAS 4a and 4b, 4b expresses only exon 4b, while 4a expresses both 4a and 4b exons. 4a and 4b code for the Hypervariable region (HVR) on the c-terminus of KRAS which is important for the regulation of KRAS through post translation modifications of the CAAX sequence[92]. It is possible that in the context of oncogenic mutation in KRAS that the two splice variants play both overlapping and mutually exclusive roles in driving tumor growth. Historically, KRAS 4b has been studied more due it being more highly expressed in cancers as well as being required for normal mouse development[93,94]. Therefore, it remains unclear if differences in the amounts of isoforms have any unique impacts on cancer biology.

Work from the Philips laboratory has shown that KRAS 4b expression is greater than 4a across several KRAS mutant cell lines using rt-qPCR probes. In contrast to cancer cell lines, colorectal patient derived cell lines had varying levels of KRAS 4a and 4b[95]. This suggest that in 2D cell culture KRAS 4b is preferred, but it is unclear if this may be the case for tumors. While the body of literature characterizing the HVR between 4a and 4b and their respective signaling outputs, it is unclear if there are any therapeutic opportunities based on which isoform is dominant in tumors.

To this end, I collaborated with the Balmain lab which generated KRAS 4a knock out (KO) cell lines, and KRAS 4b knock-down (KD) cells which alter the ration of 4a to 4b in these cells. I employed a high throughput drug screening strategy in order to determine

if there are differences in sensitivity to a large panel of clinical and tool compounds from the NCI's Informer Set drug library. I identify that KRAS 4a-expressing cells are more sensitive to MEK inhibitors, and that 4b-expressing cells are sensitive to checkpoint kinase, and PKC inhibitors. These findings are the first step in exploring the therapeutic opportunities in regards to KRAS isoform differences and provides interesting set hypothesis to test.

5.3 Results

5.3.1 A high throughput drug screen of KRAS 4a and 4b isogenic cells

For our drug screen we first characterize the growth of both A549 and SUIT2 cell lines over the course of 72 hours. I seeded cells at three different densities in 384-well format and allowed the cell proliferate for 72 hours, at which I fixed and imaged the cells for nuclei counting (see 5.4 Methods). This experiment showed that while SUIT2 KRAS 4a KO cells were able to proliferate to similar numbers as their parental counterparts, A549 4a KO cells did not grow in 384-well formats (Figure 5.1 A). With this key piece of data on hand I prioritized SUIT2 cells for HTS drug screen.

For our drug screen we used the NCI's Cancer Drug Discovery and Development (CTD^2) Informer Set that has over 300 compounds of clinical relevance. We screen using the SUIT2 cell lines, and calculated normalized AUC rations in order to rank hits between the two KRAS KO and KD cell lines (see Methods 5.4). This revealed 3 MEK inhibitors (selumetinib, rafemetinib and PD325901) to be the top hits in the 4b K.D.

background (Figure 5.1B, C). Among the top hits in the 4a K.O. cells I observed a PKC inhibitor (Go6976), two CHK inhibitors (unknown Chk2 and AZD7762), and an IKKβ inhibitor (TPCA-1) (Figure 5.1B, D). Interestingly, PKC dose response profile was among the best hits due to the 4B cell line being the most sensitive with an estimated IC_{50} value of ~0.564nM, the parental was intermediately sensitive (599nM), and the 4A KO was most resistant with an IC_{50} of 0.647nM. Take together these results highlight that there are vulnerabilities that arise once the KRAS isoforms balance is altered.

5.4 Discussion:

Efforts to target KRAS have had sobering results; however, despite these setbacks several advances have been made to better understand the RAS proteins and their role in cancer. It is becoming clear that KRAS isoform harbor unique biophysical properties that affect signaling output. My work here takes advantage of a KRAS 4a/4b isogenic platform in order to screen for therapeutic vulnerabilities. The screen uncovered that 4a-expressing cells are sensitive to MEK inhibitors, while KRAS 4B-expressing cells are sensitive to PKC, and CHK inhibitors. These findings suggest that 4a is a major driver of MAPK signaling, while 4b is dependent on PCK for upstream activation, which is consistent with previous reports showing that KRAS 4b is phosphorylated by PKC at serine 181, and disrupts the localization to the plasma and mitochondrial membrane[96]. This might explain why the 4B isoform more resistant to MEK inhibitors, since 4A protein does not have the S181 residue, and would the major isoform to spend more time in the plasma membrane where it can interact with GEF and RAF proteins to

activate MEK and ERK. We also note that CHK1 and 2 inhibitors were among the top hits in our screens, which suggest that 4b-expressing cells suffer from high stress during S, and G2-M cell cycle checkpoints. Future work will seek to test these hypotheses in larger panels of cells to elucidate the mechanism that links KRAS isoforms to these specific vulnerabilities.

5.5 Methods

5.5.1 Seeding density optimization, drug screening and AUCs calculations.

We plated 500, 750 and 1000 cells in 40 microliters in 384 well plates and allowed the cells to proliferate for 72 hours. At 72 hours cells were fixed and stained for high content imaging to count nuclei. For liquid handling each drug plate was thawed on ice, and aliquoted 3.4μL into an intermediate plate with 70μL of opti-mem to make a 0.5 mM intermediate plate. We normalized drug treated cell counts to the median of DMSO treated wells and then calculated the average of the relative cell count for each drug condition. AUCs were normalized to parental treated cells and then calculated the ratio between 4a and 4b in order to obtain a final normalized AUC ratio.

5.6 Figures

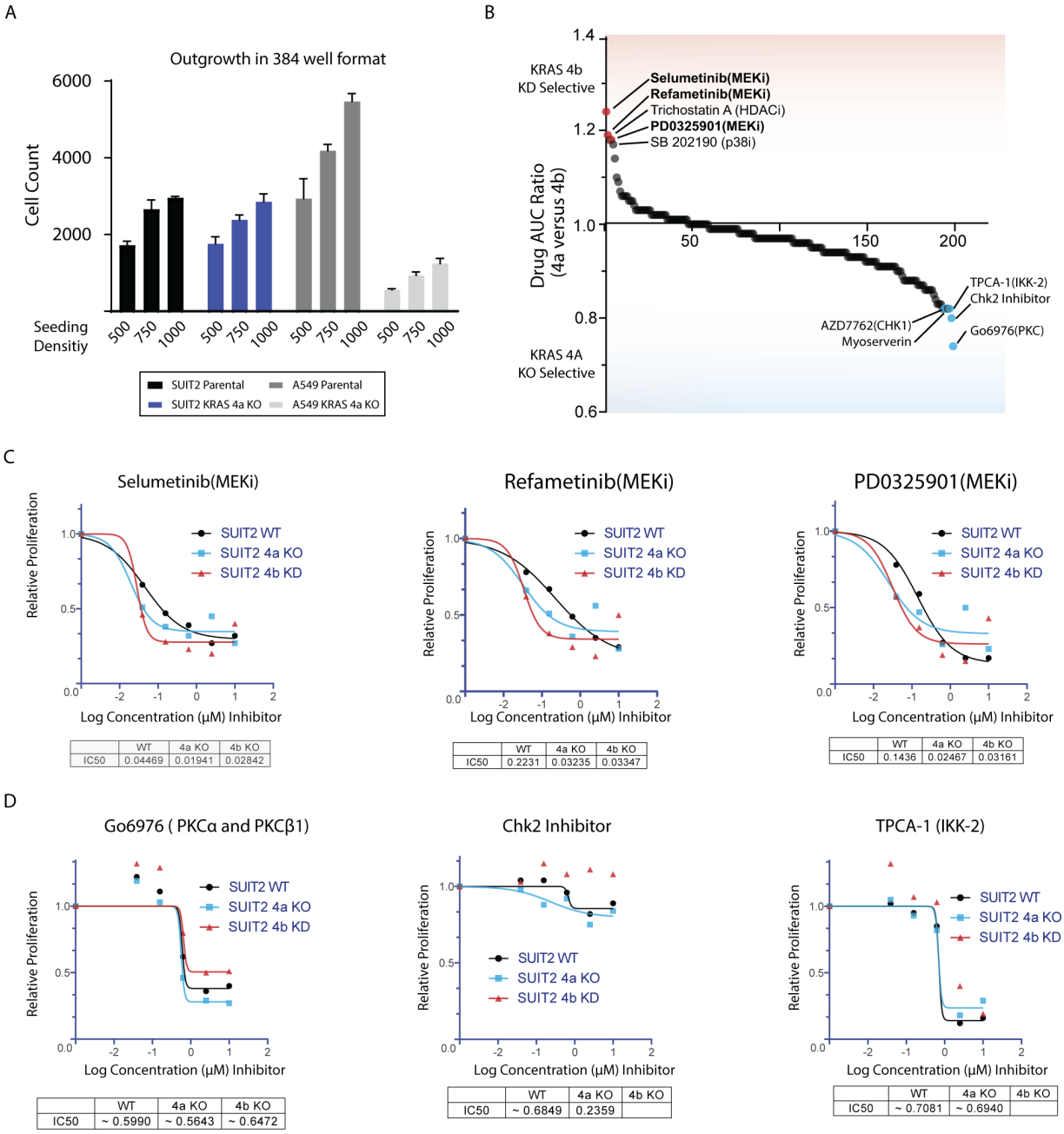

Figure 5.1 KRAS 4a and 4b Screen identifies isoform specific vulnerabilities.

(A) 72-hour outgrowth in 384-well format for KRAS 4a KO SUIT2 and A549 cells. Error bars = s.d. n=4. (B) Top hits from screen ranked by normalized AUC ratio for 4A and 4B cell lines. (C) Dose response profiles of three MEK inhibitors which were the top hits for KRAS 4b K.D. cells (D) Dose response profiles of the top three hits for the KRAS 4a KO cell lines, values represent the average of 4 replicates.

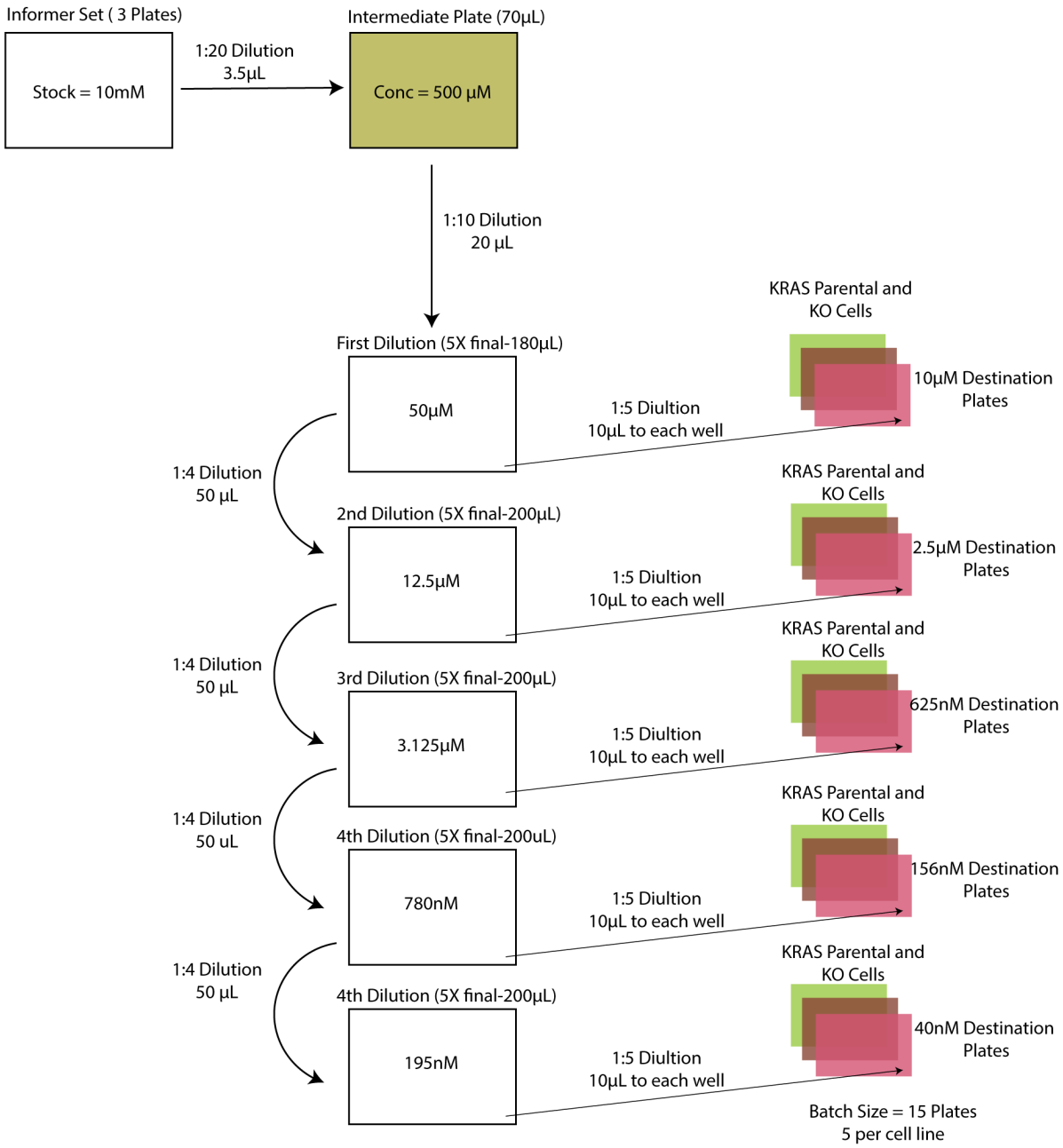

Figure 5. 2 Overview of liquid handling for KRAS 4a/4b informer set screen.

Stock Informer Set plates were thawed on ice and 3.5 µL were dispensed into a 70µL Intermediate plate, which was used to make the dilution plates for remainder of screen and any future follow up validation experiments. Cells were dose in quadruplicate 10µL per well and allowed to proliferate for 72 hours post drug exposure, upon which cells were fixed and prepared for imaging.

Bibliography

1. Lee, E. Y. H. P. & Muller, W. J. Oncogenes and Tumor Suppressor Genes. *Cold Spring Harb Perspect Biol* **2**, (2010).
2. Gainor, J. F. & Shaw, A. T. Emerging Paradigms in the Development of Resistance to Tyrosine Kinase Inhibitors in Lung Cancer. *J Clin Oncol* **31**, 3987–3996 (2013).
3. Glickman, M. S. & Sawyers, C. L. Converting cancer therapies into cures: lessons from infectious diseases. *Cell* **148**, 1089–1098 (2012).
4. Thorgeirsson, U. P. *et al.* NIH/3T3 cells transfected with human tumor DNA containing activated ras oncogenes express the metastatic phenotype in nude mice. *Mol Cell Biol* **5**, 259–262 (1985).
5. Thomas, R. K. *et al.* High-throughput oncogene mutation profiling in human cancer. *Nat. Genet.* **39**, 347–351 (2007).
6. Russo, A. *et al.* A decade of EGFR inhibition in EGFR-mutated non small cell lung cancer (NSCLC): Old successes and future perspectives. *Oncotarget* **6**, 26814–26825 (2015).
7. Bos, J. L. ras Oncogenes in Human Cancer: A Review. *Cancer Res* **49**, 4682–4689 (1989).
8. Ahearn, I. M., Haigis, K., Bar-Sagi, D. & Philips, M. R. Regulating the regulator: post-translational modification of RAS. *Nature Reviews Molecular Cell Biology* **13**, 39–51 (2012).
9. Tsimberidou, A. M., Chandhasin, C. & Kurzrock, R. Farnesyltransferase inhibitors: where are we now? *Expert Opin Investig Drugs* **19**, 1569–1580 (2010).

10. Jänne, P. A. *et al.* Selumetinib Plus Docetaxel Compared With Docetaxel Alone and Progression-Free Survival in Patients With KRAS-Mutant Advanced Non–Small Cell Lung Cancer: The SELECT-1 Randomized Clinical Trial. *JAMA* **317**, 1844–1853 (2017).
11. Jokinen, E. & Koivunen, J. P. MEK and PI3K inhibition in solid tumors: rationale and evidence to date. *Ther Adv Med Oncol* **7**, 170–180 (2015).
12. Kaelin, W. G. The concept of synthetic lethality in the context of anticancer therapy. *Nat. Rev. Cancer* **5**, 689–698 (2005).
13. Farmer, H. *et al.* Targeting the DNA repair defect in *BRCA* mutant cells as a therapeutic strategy. *Nature* **434**, 917–921 (2005).
14. Swisher, E. M. *et al.* Rucaparib in relapsed, platinum-sensitive high-grade ovarian carcinoma (ARIEL2 Part 1): an international, multicentre, open-label, phase 2 trial. *Lancet Oncol.* **18**, 75–87 (2017).
15. Kaufman, B. *et al.* Olaparib Monotherapy in Patients With Advanced Cancer and a Germline BRCA1/2 Mutation. *J Clin Oncol* **33**, 244–250 (2015).
16. Costa-Cabral, S. *et al.* CDK1 Is a Synthetic Lethal Target for KRAS Mutant Tumours. *PLoS ONE* **11**, e0149099 (2016).
17. Luo, J. *et al.* A Genome-wide RNAi Screen Identifies Multiple Synthetic Lethal Interactions with the Ras Oncogene. *Cell* **137**, 835–848 (2009).
18. Scholl, C. *et al.* Synthetic Lethal Interaction between Oncogenic KRAS Dependency and STK33 Suppression in Human Cancer Cells. *Cell* **137**, 821–834 (2009).

19. Steckel, M. *et al.* Determination of synthetic lethal interactions in KRAS oncogene-dependent cancer cells reveals novel therapeutic targeting strategies. *Cell Res* **22**, 1227–1245 (2012).
20. Barbie, D. A. *et al.* Systematic RNA interference reveals that oncogenic KRAS-driven cancers require TBK1. *Nature* **462**, 108–112 (2009).
21. Kumar, M. S. *et al.* The GATA2 Transcriptional Network Is Requisite for RAS Oncogene-Driven Non-Small Cell Lung Cancer. *Cell* **149**, 642–655 (2012).
22. Downward, J. RAS Synthetic Lethal Screens Revisited: Still Seeking the Elusive Prize? *Clin Cancer Res* **21**, 1802–1809 (2015).
23. Ryan, C. J., Bajrami, I. & Lord, C. J. Synthetic Lethality and Cancer - Penetrance as the Major Barrier. *Trends Cancer* **4**, 671–683 (2018).
24. Rao, D. D., Vorhies, J. S., Senzer, N. & Nemunaitis, J. siRNA vs. shRNA: similarities and differences. *Adv. Drug Deliv. Rev.* **61**, 746–759 (2009).
25. Rao, D. D., Senzer, N., Cleary, M. A. & Nemunaitis, J. Comparative assessment of siRNA and shRNA off target effects: what is slowing clinical development. *Cancer Gene Therapy* **16**, 807–809 (2009).
26. Theis, M. & Buchholz, F. MISSION esiRNA for RNAi Screening in Mammalian Cells. *J Vis Exp* (2010). doi:10.3791/2008
27. Gilbert, L. A. *et al.* CRISPR-mediated modular RNA-guided regulation of transcription in eukaryotes. *Cell* **154**, 442–451 (2013).
28. Zhang, X.-H., Tee, L. Y., Wang, X.-G., Huang, Q.-S. & Yang, S.-H. Off-target Effects in CRISPR/Cas9-mediated Genome Engineering. *Molecular Therapy - Nucleic Acids* **4**, e264 (2015).

29. Sun, C. *et al.* Intrinsic Resistance to MEK Inhibition in KRAS Mutant Lung and Colon Cancer through Transcriptional Induction of ERBB3. *Cell Reports* **7**, 86–93 (2014).
30. Kitai, H. *et al.* Epithelial-to-Mesenchymal Transition Defines Feedback Activation of Receptor Tyrosine Kinase Signaling Induced by MEK Inhibition in KRAS-Mutant Lung Cancer. *Cancer Discov* **6**, 754–769 (2016).
31. Hu, H.-M. *et al.* A Quantitative Chemotherapy Genetic Interaction Map Reveals Factors Associated with PARP Inhibitor Resistance. *Cell Rep* **23**, 918–929 (2018).
32. Zimmermann, M. *et al.* CRISPR screens identify genomic ribonucleotides as a source of PARP-trapping lesions. *Nature* **559**, 285 (2018).
33. Torrance, C. J., Agrawal, V., Vogelstein, B. & Kinzler, K. W. Use of isogenic human cancer cells for high-throughput screening and drug discovery. *Nature Biotechnology* **19**, 940–945 (2001).
34. Stolze, B., Reinhart, S., Bulllinger, L., Fröhling, S. & Scholl, C. Comparative analysis of KRAS codon 12, 13, 18, 61, and 117 mutations using human MCF10A isogenic cell lines. *Sci Rep* **5**, 8535 (2015).
35. Martins, M. M. *et al.* Linking Tumor Mutations to Drug Responses via a Quantitative Chemical–Genetic Interaction Map. *Cancer Discovery* **5**, 154–167 (2015).
36. Yamori, T. Panel of human cancer cell lines provides valuable database for drug discovery and bioinformatics. *Cancer Chemother. Pharmacol.* **52 Suppl 1**, S74-79 (2003).
37. Yang, W. *et al.* Genomics of Drug Sensitivity in Cancer (GDSC): a resource for therapeutic biomarker discovery in cancer cells. *Nucleic Acids Res.* **41**, D955-961 (2013).

38. Daemen, A. *et al.* Modeling precision treatment of breast cancer. *Genome Biol* **14**, R110 (2013).
39. Barretina, J. *et al.* The Cancer Cell Line Encyclopedia enables predictive modeling of anticancer drug sensitivity. *Nature* **483**, 603–607 (2012).
40. Haverty, P. M. *et al.* Reproducible pharmacogenomic profiling of cancer cell line panels. *Nature* **533**, 333–337 (2016).
41. Ashworth, A. & Lord, C. J. Synthetic lethal therapies for cancer: what's next after PARP inhibitors? *Nature Reviews Clinical Oncology* 1 (2018). doi:10.1038/s41571-018-0055-6
42. Rancati, G., Moffat, J., Typas, A. & Pavelka, N. Emerging and evolving concepts in gene essentiality. *Nature Reviews Genetics* **19**, 34–49 (2018).
43. Bandyopadhyay, S. *et al.* Rewiring of Genetic Networks in Response to DNA Damage. *Science* **330**, 1385–1389 (2010).
44. Bryant, H. E. *et al.* Specific killing of BRCA2-deficient tumours with inhibitors of poly(ADP-ribose) polymerase. *Nature* **434**, 913–917 (2005).
45. Ashworth, A., Lord, C. J. & Reis-Filho, J. S. Genetic Interactions in Cancer Progression and Treatment. *Cell* **145**, 30–38 (2011).
46. Kim, H. S. *et al.* Systematic Identification of Molecular Subtype-Selective Vulnerabilities in Non Small Cell Lung Cancer. *Cell* **155**, (2013).
47. Kim, J. *et al.* XPO1-dependent nuclear export is a druggable vulnerability in KRAS-mutant lung cancer. *Nature* **advance online publication**, (2016).
48. Fröhling, S. & Scholl, C. STK33 Kinase Is Not Essential in KRAS-Dependent Cells–Letter. *Cancer Research* **71**, 7716–7716 (2011).

49. Tessema, M. *et al.* GATA2 is epigenetically repressed in human and mouse lung tumors and is not requisite for survival of KRAS mutant lung cancer. *J Thorac Oncol* **9**, 784–793 (2014).
50. Christodoulou, E. G. *et al.* Detection of COPB2 as a KRAS synthetic lethal partner through integration of functional genomics screens. *Oncotarget* **8**, 34283–34297 (2017).
51. Collins, S. R. *et al.* Functional dissection of protein complexes involved in yeast chromosome biology using a genetic interaction map. *Nature* **446**, 806–810 (2007).
52. Costanzo, M. *et al.* The genetic landscape of a cell. *Science* **327**, 425–431 (2010).
53. Galardini, M. *et al.* The impact of the genetic background on gene deletion phenotypes in Saccharomyces cerevisiae. *bioRxiv* 487439 (2018). doi:10.1101/487439
54. Lord, C. J. & Ashworth, A. BRCAness revisited. *Nat. Rev. Cancer* **16**, 110–120 (2016).
55. Lee, I., Blom, U. M., Wang, P. I., Shim, J. E. & Marcotte, E. M. Prioritizing candidate disease genes by network-based boosting of genome-wide association data. *Genome Res.* **21**, 1109–1121 (2011).
56. Ruepp, A. *et al.* CORUM: the comprehensive resource of mammalian protein complexes—2009. *Nucleic Acids Research* **38**, D497–D501 (2010).
57. Bader, G. D. & Hogue, C. W. An automated method for finding molecular complexes in large protein interaction networks. *BMC Bioinformatics* **4**, 2 (2003).
58. Ding, L. *et al.* Somatic mutations affect key pathways in lung adenocarcinoma. *Nature* **455**, 1069–1075 (2008).

59. Modrek, B. *et al.* Oncogenic activating mutations are associated with local copy gain. *Mol. Cancer Res.* **7**, 1244–1252 (2009).

60. Roguev, A. *et al.* Quantitative genetic-interaction mapping in mammalian cells. *Nat Meth* **10**, 432–437 (2013).

61. Boone, C., Bussey, H. & Andrews, B. J. Exploring genetic interactions and networks with yeast. *Nat. Rev. Genet.* **8**, 437–449 (2007).

62. Guarente, L. Synthetic enhancement in gene interaction: a genetic tool come of age. *Trends Genet.* **9**, 362–366 (1993).

63. Costanzo, M. *et al.* A global genetic interaction network maps a wiring diagram of cellular function. *Science* **353**, (2016).

64. McGillicuddy, N., Floris, P., Albrecht, S. & Bones, J. Examining the sources of variability in cell culture media used for biopharmaceutical production. *Biotechnol. Lett.* **40**, 5–21 (2018).

65. Stein, A. Decreasing variability in your cell culture. *BioTechniques* **43**, 228–229 (2007).

66. Settleman, J., Sawyers, C. L. & Hunter, T. Challenges in validating candidate therapeutic targets in cancer. *eLife* **7**, e32402 (2018).

67. Babij, C. *et al.* STK33 kinase activity is nonessential in KRAS-dependent cancer cells. *Cancer Res.* **71**, 5818–5826 (2011).

68. Luo, T. *et al.* STK33 kinase inhibitor BRD-8899 has no effect on KRAS-dependent cancer cell viability. *Proc. Natl. Acad. Sci. U.S.A.* **109**, 2860–2865 (2012).

69. Murai, J. *et al.* Trapping of PARP1 and PARP2 by Clinical PARP Inhibitors. *Cancer Res.* **72**, 5588–5599 (2012).

70. Balmain, A., Ramsden, M., Bowden, G. T. & Smith, J. Activation of the mouse cellular Harvey-ras gene in chemically induced benign skin papillomas. *Nature* **307**, 658–660 (1984).
71. Bonham, K. *et al.* Activation of the cellular Harvey ras gene in mouse skin tumors initiated with urethane. *Mol. Carcinog.* **2**, 34–39 (1989).
72. Wang, H., La Russa, M. & Qi, L. S. CRISPR/Cas9 in Genome Editing and Beyond. *Annu. Rev. Biochem.* **85**, 227–264 (2016).
73. Ben-David, U. *et al.* Genetic and transcriptional evolution alters cancer cell line drug response. *Nature* **560**, 325–330 (2018).
74. Yam, A. Y. *et al.* Defining the TRiC/CCT interactome links chaperonin function to stabilization of newly made proteins with complex topologies. *Nat. Struct. Mol. Biol.* **15**, 1255–1262 (2008).
75. Sun, C. *et al.* Rational combination therapy with PARP and MEK inhibitors capitalizes on therapeutic liabilities in RAS mutant cancers. *Sci Transl Med* **9**, (2017).
76. Gilad, O. *et al.* Combining ATR suppression with oncogenic Ras synergistically increases genomic instability, causing synthetic lethality or tumorigenesis in a dosage-dependent manner. *Cancer Res* **70**, 9693–9702 (2010).
77. Kalimutho, M. *et al.* Enhanced dependency of KRAS-mutant colorectal cancer cells on RAD51-dependent homologous recombination repair identified from genetic interactions in Saccharomyces cerevisiae. *Mol Oncol* **11**, 470–490 (2017).
78. Kotsantis, P. *et al.* Increased global transcription activity as a mechanism of replication stress in cancer. *Nat Commun* **7**, 13087 (2016).

79. R Core Team. R: The Hypergeometric Distribution. *The Hypergeometric Distribution* (2018). Available at: https://stat.ethz.ch/R-manual/R-devel/library/stats/html/Hypergeometric.html. (Accessed: 11th January 2019)
80. Reimand, J. *et al.* g:Profiler-a web server for functional interpretation of gene lists (2016 update). *Nucleic Acids Res.* **44**, W83-89 (2016).
81. Benjamini, Y. & Hochberg, Y. Controlling the False Discovery Rate: A Practical and Powerful Approach to Multiple Testing. *Journal of the Royal Statistical Society. Series B (Methodological)* **57**, 289–300 (1995).
82. Hanahan, D. & Weinberg, R. A. Hallmarks of cancer: the next generation. *Cell* **144**, 646–674 (2011).
83. Hengel, S. R., Spies, M. A. & Spies, M. Small-Molecule Inhibitors Targeting DNA Repair and DNA Repair Deficiency in Research and Cancer Therapy. *Cell Chemical Biology* **24**, 1101–1119 (2017).
84. Grabocka, E. *et al.* Wild-type H- and N-Ras promote mutant K-Ras driven tumorigenesis by modulating the DNA damage response. *Cancer Cell* **25**, 243–256 (2014).
85. Hafner, M., Niepel, M., Chung, M. & Sorger, P. K. Growth rate inhibition metrics correct for confounders in measuring sensitivity to cancer drugs. *Nat. Methods* **13**, 521–527 (2016).
86. Subramanian, A. *et al.* Gene set enrichment analysis: A knowledge-based approach for interpreting genome-wide expression profiles. *PNAS* **102**, 15545–15550 (2005).
87. Zhao, W. *et al.* BRCA1-BARD1 promotes RAD51-mediated homologous DNA pairing. *Nature* **550**, 360–365 (2017).

88. Singh, A. *et al.* A Gene Expression Signature Associated with “K-Ras Addiction” Reveals Regulators of EMT and Tumor Cell Survival. *Cancer Cell* **15**, 489–500 (2009).
89. Janes, M. R. *et al.* Targeting KRAS Mutant Cancers with a Covalent G12C-Specific Inhibitor. *Cell* **172**, 578-589.e17 (2018).
90. Clark, N. A. *et al.* GRcalculator: an online tool for calculating and mining dose-response data. *BMC Cancer* **17**, 698 (2017).
91. Guzmán, C., Bagga, M., Kaur, A., Westermarck, J. & Abankwa, D. ColonyArea: An ImageJ Plugin to Automatically Quantify Colony Formation in Clonogenic Assays. *PLOS ONE* **9**, e92444 (2014).
92. Laude, A. J. & Prior, I. A. Palmitoylation and localisation of RAS isoforms are modulated by the hypervariable linker domain. *J Cell Sci* **121**, 421–427 (2008).
93. Plowman, S. J. *et al.* K-ras 4A and 4B are co-expressed widely in human tissues, and their ratio is altered in sporadic colorectal cancer. *J. Exp. Clin. Cancer Res.* **25**, 259–267 (2006).
94. Plowman, S. J. *et al.* While K-ras Is Essential for Mouse Development, Expression of the K-ras 4A Splice Variant Is Dispensable. *Mol Cell Biol* **23**, 9245–9250 (2003).
95. Tsai, F. D. *et al.* K-Ras4A splice variant is widely expressed in cancer and uses a hybrid membrane-targeting motif. *PNAS* **112**, 779–784 (2015).
96. Bivona, T. G. *et al.* PKC regulates a farnesyl-electrostatic switch on K-Ras that promotes its association with Bcl-XL on mitochondria and induces apoptosis. *Mol. Cell* **21**, 481–493 (2006).

Publishing Agreement

It is the policy of the University to encourage the distribution of all theses, dissertations, and manuscripts. Copies of all UCSF theses, dissertations, and manuscripts will be routed to the library via the Graduate Division. The library will make all theses, dissertations, and manuscripts accessible to the public and will preserve these to the best of their abilities, in perpetuity.

Please sign the following statement:

I hereby grant permission to the Graduate Division of the University of California, San Francisco to release copies of my thesis, dissertation, or manuscript to the Campus Library to provide access and preservation, in whole or in part, in perpetuity.

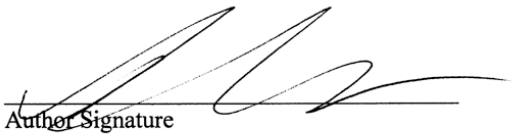

Author Signature

3/28/19

Date